ELECTROPLASTIC CUTTING INFLUENCE IN MACHINING PROCESSES

A dissertation submitted to
the Universitat Politècnica de Catalunya for the
degree of Doctor of Philosophy in Mechanical Engineering

Saqib Hameed

Thesis director: Hernán Alberto González Rojas

May 2017

Department of Mechanical Engineering
Universitat Politècnica de Catalunya

Contents

List of Figures

List of Tables

Foreword

The aim of this thesis is to report the electroplastic cutting effect in machining operations. The effect of electropulses has beed studied in drilling and round turning processes. A mechanism was developed in the form of electrically isolated system for each process to perform the investigations under safe mode. The main objective was to study the machinability differences between conventional and electrically assisted metal cutting processes.

For this, an electropulse generator was used to assist the machining processes through electrical connectors between the workpiece and cutting tool. Before start of experiments, it was made sure that the machine tools were completely isolated from electricity to perform experiments under safe and controlled environment. The experiments were conducted by using current pulses of short duration through different metallic materials with different cutting parameters during cutting processes. The results obtained then compared to study the machinability differences between conventional and non conventional processes. The machinability of materials is analyzed by comparing the power consumption, chip compression ratio and effect of current densities during machining processes. It was found that the process efficiency improved when current density passed through cutting materials. However, it was also noted that the effect of high current densities changes the behaviour of materials which is difficult to understand and for that it is necessary to study the numerical analysis and metallography of metallic materials.

The metal cutting processes (drilling and round turning) were carried out in the manufacturing laboratory of Universitat Politècnica de Catalunya (Spain). Finally, the research will provide a valuable resource for scientists seeking background information about electroplastic metal cutting processes.

Acknowledges

The completion of my dissertation and subsequent PhD has been long journey. My dissertation has always been a priority, but as most know, there are several priorities in person's life at one time. Unfortunately, due to different challenges in my life it was not easy to concentrate and give full attentions for completing my dissertation. Many have doubted about my commitment if I can finish my dissertation in time but I have decided that I will complete my PhD in my own time and my own terms.

First of all I would like to express my sincere gratitude and special appreciation to my thesis advisor professor Dr. Hernán Alberto González Rojas. Thanks for considering me and believe in me to take part in such a challenging project. His support, research motivation, patience, valuable guidance and most important his grip on understanding of project have been priceless. I could not have imagined having a better advisor and mentor for PhD study. His door was always opened for me whenever I needed some assistance and guideline or had a question about my research, his consistency steered me in right direction. Also I would like to thanks to the Departament d'Enginyeria Mecànica, Universitat Politècnica de Catalunya by the financial support through the grant Projectes de reserca del DEM-2015.

Though my name is alone on front cover of this thesis but I am not only contributor. There are number of people behind this piece of work who deserved to be acknowledged here. Firstly, I would like to thank my colleagues and sincere friends Antonio Sànches Egea and Fayyaz Ahmad for their unconditional support and suggestions at various points of my research programme.

Finally I must express my very profound gratitude to my inspiring mother and generous father, my brothers Amjad, Wasim and Aqib. Inspite of long distance, they have supported me and remained loyal to me through thick and thin. Your complete and unconditional love carries me through always.

I would like to thank my wife for her unremitting encouragement and patience. I still have not found the words that describe or express how I feel for this woman and what her presence in my life has meant. Thank you for making me more than I am.

Chapter 1

Introduction

The phenomenon of electroplasticity has been demostrated to reduce the flow stresses of deformed materials to attain better properties, deformability and machinability by applying the electropulses (EPs) of short durations and high density in the deformation zone, while at the same time microstructure improved and plasticity increases significantly [1]. This influence of the electric current pulses on the plastic flow is called the electroplastic effect. It was first discovered and reported by Troistkii and Likhtman in 1963, investigating the influence of drift electrons on the flow stress in a variety of metals [2].

H. Conrad et al. [3] reviewed the influence of an electric field or corresponding current on the plastic deformation of metals and ceramics. They studied that high density dc current applied either continuosly or as short duration pulses can reduce the flow stress and significantly increase the plastic deformation rate in metals, but more importantly retarted cavitation and grain growth. Hui et al. [4] investigated the effect of EPs on dislocation mobility and demonstrated that the electropulsing treatment can decrease dislocation tangles and enhance dislocation mobility. H. Conrad et al. [5] showed that the dislocation movement leads to the modification of the material's lattice, changing the dimensions of interstitial gaps. Such lattice variation brings changes in the mechanical properties of material.

Electroplastic effects

The mechanism about electropulsing on the microstructure of materials is not very clear. Although the researches on electroplasticity phenomenon are fruitful but still there are some important issues concerning the side effects such as thermal, pinch and skin effects, electron wind effects and thermal compressive stress occur in concert with the direct effect caused by the electrical current. The role of these effects is an important issue in electroplasticity.

Skin and pinch effects:

The skin effect is associated near a specimen surface when a high frequency current is applied. The depth δ of skin effect can be calculated as suggested by Okazaki et al. [6]:

$$\delta = \left(\frac{\pi \cdot f \cdot \mu}{\rho} \right)^{-1/2} \tag{1.1}$$

Where f is frequency of pulses, μ is permeability, and ρ is the resisitivity of material. Conrad and coworkers [7] investigated that the current distribution is uniform throughout the cross section of material rather than at the surface. The pinch effect occurs by applying high current pulses producing radial compressive stress which can be estimated as follows:

$$\delta = \nu \cdot \mu \cdot J^2 \cdot \frac{a^2}{2} 2 \tag{1.2}$$

Where μ is the Poisson's ratio, a is the specimen radius and J is the current density. Okazaki et al. [6] found that the contributions from the skin and pinch effects associated with current pulses are quite small compared with the total stress changes due to the plastic deformation of materials. However, these stresses can enhance the atomic mobility and reduce the strength of obstacles opposing the dislocation motion.

Heating effects:

The heating effect is ascribed to Joule law. The average temperature rise by Joule heating effect can be regarded as adiabatic due to very short time during electroplastic treatment (EPT). The thermal effect of EPs plays an important role in the reduction of deformation resistance and improvement of plasticity [6]. The equation for single current pulse which can produce adiabatic temperature rise can be written as follows:

$$\Delta T = \frac{\rho J^2 t_p}{c_p d} \tag{1.3}$$

Where ρ is the total resistivity, t_p is the pulse duration, J is the current density, c_p is the specific heat and d is the density of material.

Tang et al. [8] observed that an adequate thermal effect resulting from the Joule heating effect of EPT is necessary to increase the nucleation rate of recrystallization. Hui et al. [9] stated that When EPs are passed through the metal specimen, the temperature rise is higher in the area with defects than those without defects due to inhomogeneous resistivity in the metal. This inhomogeneous rise of temperature causes inhomogeneous thermal expansion and the defected area suffers compressive stresses as compared to area without defects.

Due to very short duration of EPs, the material particles undergo heavy stress impact [10]. Because of increase of current density, a higher temperature would be

produced and hence maximum stresses would be produced. Then, based on the hight rate heating of EPs, the maximum thermal stress suggested by Tang et al. [11] can be calculated as follows:

$$\sigma_{max} = E \cdot \alpha \cdot \Delta T \tag{1.4}$$

where E is Young's modulus and α is the coefficient of thermal expansion.

Jiang et al. [12] studied that as compared to conventional heat treatment, the EPT can increase sub grain growth speed by improving climb velocity of dislocation due to enhancement of atomic diffusion, which is resulting from the coupling action of thermal and athermal effects. They also observed that at low temperature, the recrystallization does not occur even with the coupling of thermal and athermal effects because Joule heating effect is not enough. The exact mechanism of athermal effect is still not very clear and there is possibility that it results from additional force of electron called electron wind as explained below.

Electron wind effects:

The drift electrons pushed on dislocations when high density EP have passed through the specimen, the force is called electron wind force which is proportional to the current density. The electron wind force for metal single crystals can be estimated by the following equation [6].

$$F_{ew} = en_eJ\left(\frac{\rho}{N_D}\right) \tag{1.5}$$

Where F_{ew} is electron wind force per unit dislocation length, (ρ/N_D) is the specific resistivity per unit dislocation length, N_D dislocation density and n_e is the electron density.

The tremendous force is impacted due to very short duration of EPs which further enhances irregular speed of atoms based on thermal effect. As the electron wind force increases the higher athermal effects will be induced due to higher values of current density [13]. The athermal effects strongly depend on the electrical parameters such s frequency f, pulse duration t_p and high current density J. The increase of these parameters not only enhancing athermal effects but also increases the thermal effects [12]. Qing et al. [14] observed that EPs enhance recrystallization due to the joint action of the accumulation and annihilation effects at relatively low temperature. They proposed that the electron wind force accumulates dislocations which form the coarse grain boundaries. The coupling of the thermal and athermal (electromigration) effects annihilate dislocations. Hence, effect of EPs consist of two parts: the accumulation effect induced by the electron wind force and annihilation effect caused by the coupling action of the thermal and athermal effects.

Conrad and coworkers [3] reported that increase of material plastic flow is found mainly by the direct effect of the drift electrons on dislocation motion. The electron wind force reduces dislocation density and increase the mobility of dislocation which enhances the nucleation rate of recrystallization. Hui et al. [9] reported that EPT enhances the migration of atoms and minimizes the strength of obstacles which oppose dislocation motion. The low residual dislocation density within the newly formed grains shows that stored energy is decreased. They also noted that the retardation of subsequent grain growth is due to the reduction in driving force for the growth of newly crystallized grains and hence finally smaller crystallized grains can be obtained. Molotskii and Fleurov [15] observed that electron wind force is too small to produce plastic deformation in the material during EPT. They reported that the magnetic field induced by EPs is the major reason for the occurrence of electroplasticity phenomenon.

Although the contributions of side effects and electron wind force are negligible due to low temperature of EPT. Hence an adequate thermal effect from Joule heating is necessary for substantially accelerating recystallization in materials subjected to EPT.

oxidation reduction:

Rufei et al. [16] proved that electropulses plays a vital role in improving the surface finish by reducing the surface oxides during EPT. Toe et al. [17] proposed that oxidation can be expressed as,

$$\left(\frac{\Delta W}{A}\right)^{n} = K_t + C \tag{1.6}$$

Where ΔW is the mass difference before and after oxidation, A is the area, n is the index number of oxidation rate, k_n is the coefficient of oxidation velocity, t is the time and c is the constant.

The Eq. 1.6 shows that the metals will have more oxidation on the surface at high temperatures for longer time. Thus, the time for metals at high temperature should be reduced and eventually, EPs can decrease the heat treatment time of the process.

The role of the side effects such as thermal, pinch and skin effects is an important issue but still they are far from explaining the observed phenomenon. Several mechanisms have been proposed to explain the combined thermal and athermal effects arising from electropulsing.

Mechanisms of electroplasticity

The mechanism of electroplasticity is mainly based on the effect of electric current

on dislocation propagation. Xu et al. [18] proposed that the dynamic recrystallization occurs due to the combined thermal and athermal effects arising from electroplasticity at relatively low temperature. The momentum from electrons gives an additional high energy input which enhances the propagation of dislocations. Jiang et al. [19] indicated that propagation of dislocation climb into sub grain boundaries is due to the substantial increase in the atomic flux resulted from the coupling action of the thermal and athermal effects as can be described by the following equation:

$$J_t = \frac{pi \cdot G \cdot b \cdot D_l}{(1-\nu) \cdot k \cdot T} \tag{1.7}$$

$$J_a = \frac{2N \cdot D_l \cdot Z^* \cdot e \cdot \rho \cdot f \cdot j_m \cdot t_p}{(1-\nu) \cdot k \cdot T} \tag{1.8}$$

$$J = J_t + J_a = \frac{pi \cdot G \cdot b \cdot D_l}{(1-\nu) \cdot k \cdot T} + \frac{2N \cdot D_l \cdot Z^* \cdot e \cdot \rho \cdot f \cdot j_m \cdot t_p}{(1-\nu) \cdot k \cdot T} \tag{1.9}$$

Where J is the total flux of atom under EPT, J_t is the thermal atomic flux of atom, J_a is the flux of atom by athermal effect, G is the shear modulus, b the burger vector, ν is the Poisson ratio, N is the density of atom, Z is effective valence of the Mg ion, e is the charge on electron, ρ is the electrical resistivity, k is the Boltzmann constant, T is the absolute temperature, D_l is the lattice diffusion coefficient, j_m is the peak current density, f is frequency and t_p is the duration of EPs.

Accordingly, the thermal effects can be expressed by high rise of temperature due to Joule heating effect and athermal effect results from tremendous force between electrons and atoms (electron wind). The Eq. 1.9 shows that by increasing f, t_p and j_m not only increases the athermal effect but also increases the thermal effect, because of increasing j_m , f and t_p results in large joule heating effect. Thus, the temperature is an important factor for the atomic flux and accelerating the recrystallization behaviour. There is a possibility that without the aid of thermal effect, the contribution of athermal effects to accelerate dislocation climb and sub grain growth is so small that recrystallization does not occur during EPT [1].

Generally, during plastic deformation of material, the distribution of defects such as microcracks, cavity and void is not same and electrical resistivity is higher in the area with defects than that without defects. When the high density EPs are passed through the metal, the change of temperature is higher in the area with defects because of the joule heating and thermal compressive stresses. Accordingly, thermal and athermal effects are higher in the area with defects because of the big regional resistivity and strong influence of the the current pulses. This is termed as the "*Selective effect*" of electroplasticity [20]. During electropulsing, the influence of thermal and athermal effects on compressive stress variation gives rise an additional driving force as follows:

$$\Delta P = P_{th} + P_{ath} \tag{1.10}$$

Where,

$$P_{th} = \left(\frac{2a \cdot \Delta S \cdot gradT}{\varphi}\right) \tag{1.11}$$

$$P_{ath} = \left(\frac{\rho D}{N_D} \cdot e \cdot n_e \cdot j\right) \tag{1.12}$$

The Eq. 1.10 can be written as;

$$\Delta P = \left(\frac{2a \cdot \Delta S \cdot gradT}{\varphi}\right) + \left(\frac{\rho D}{N_D} \cdot e \cdot n_e \cdot j\right) \tag{1.13}$$

where ΔS is the difference in the entropy between the grain boundary and crystal (approximately equal to entropy of melting), φ is the atomic volume, 2a is the thickness of the grain boundary, gradT is the temperature gradient, $\rho D/N_D$ is the specific resistivity per unit dislocation length, n_e is the electron density, N_D is the dislocation density, and j is the current density.

The results from Eq. 1.13 indicated that by increasing current density j, the substantial thermal and athermal effects are produced which increases the velocity of moving boundaries during EPT at relatively low temperature.

Furthermore, the EPs can change the physical properties of materials by changing the phase transformation due to difference in crystal structures. Hui et al. [21] concluded that fine and homogeneous microstructures can be obtained when the materials are treated by EPs. The electropulsing treatment tremendously accelerates phase transformation in two stages [22]: The first stage is quenching from supersaturated state approaching the final stable state and the second stage is upquenching from the final stable state to a higher temperature state. They investigated that as compared to conventional processes, the phase transformations are faster in the way of quenching than the reverse phase transformation in upquenching during EPT. The mechanism of electropulsing induced phase transformation from the point of view of Gibbs free energy consists of various parts: chemical Gibbs free energy, strain energy, surface energy, the Gibbs free energy induced by crystal orientation, the Gibbs free energy induced by EPs and so on as follows:

$$\Delta G = \Delta G_{chem.} + \Delta G_{stress} + \Delta G_{surf.} + \Delta G_{orient.} + \Delta G_{ep} + ... \tag{1.14}$$

From the thermodynamic point of view, the chemical Gibbs free energy, $\Delta G_{chem.}$ is considered as the main part of driving force. The strain energy, ΔG_{stress} induces various internal deformation energies that may be available due to thermal stress during solidification of melt and external deformation energies. EPs increase the Gibbs free energy, ΔG_{ep} which ultimately increases the total driving force for the phase transformation. Zhang et al. [23] reported that during electropulsing new structural distortions such as

vacancies and dislocations are produced in the material which reduces the Gibbs free energy, ΔG_{ep} due to the interaction between electrons and dislocations and vacancies. Accordingly, the Gibbs free energy, ΔG_{ep} for the reverse transformation are also reduced.

Hence, due to the increase of current density j_m, an adequate thermal and athermal effects are produced due to the increase of P_{ath} and P_{th}. The contribution of thermal effects resulting from Joule heating effect of EPT should be sufficient to enhance athermal effects resulting from movement of electrons. Consequently, the phase transformation occurs due to high stored energy and faster grain boundary growth at relatively low temperature. Despite the recent progress, the mechanism of electropulsing on the phase transformation, electromigration and mechanical and metallurgical variations is still inadequate. Further systematic studies are required to explain the influence of current pulses on these phenomena.

Moreover, electroplasticity is one of the most effective ways to simplify the manufacturing processes while enhancing the properties of final product. Yao et al. [24] presented that the wire drawing force and ultimate tensile strength are significantly reduced while ductility and surface quality improved by applying current pulses in wire drawing process of an austenitic stainless steel. Tang et al. [8] [25] demonstrated that electroplastic process can decrease the drawing stress by about 20-50 %, increase the plasticity and improve the surface quality in the cold drawing of stainless steel wire. They also described that the tensile strength and resistivity of the wire have decreased which lead to a considerable reduction of the drawing force [26]. Numerous studies have proved that electroplsaticity has a direct industrial impact as reported by Xu et al. [13] that the phenomenon of electroplasticity improves the ductility and surface quality of AZ31 Mg alloy strips during rolling process by releasing the intensity of stress induced by twinning and slip of the coarse grains. Hui et al. [9] studied the effect of high density EPT on formability of TC4 titanium alloy sheet and the experimental results indicated that electropulsing significantly changes the mechanical properties of metal sheet by reducing the yield stress upto 19.8 % and elongation is increased by 35 %. They also found that due to the effect of EPs in titanium alloy sheets, the dislocation tangles decreased and dislocation mobility enhanced with maximum current density of 7.9 kA/mm^2 and pulse period of 110 μs [4].

Electroplastic effect on power consumption

Reduction in energy consumption can contribute to improve the manufacturing quality during material removal processes. In drilling process, the material removal rate (MRR) is greatly influenced by cutting speed, feed rate and drill diameter and the energy consumption decreased with increase in MRR [29]. Therefore, if it is desired to increase the productivity for a given material, then the cutting speed, feed rate,

tool geometry and tool material should be selected properly to achieve optimum drill performance.

The investigations showed that the MRR plays a decisive role in determining machine energy consumption. When the MRR increased, the energy required by machine reduced and its efficiency increased [30]. Simoneau et al. [31] realized that by increasing spindle speed and feed rates, MRR increases which can lead to an overall energy consumption decrease. Bhattacharya et al. [32] investigated the effects of cutting parameters on power consumption during high speed machining of AISI 1045 steel. They found that cutting speed was observed to be the most significant factor to reduce the power consumption with a contribution of 77.4%, followed by depth of cut (13.2%). Fernandez-Abia et al. [33] analyzed the effect of high cutting speeds over cutting forces, surface quality and chip geometry during turning process. They concluded that when the cutting speed increases, the three force components reduce and then they increase again with cutting speed as shown in Fig. 1.1. They also observed that the main component (tangential component) of cutting forces reduces at high speeds, which implies less power consumption and less stress and deformation in cutting tool. While, the chip thickness is significantly less, which implies low chip compression ratio and higher shear angles.

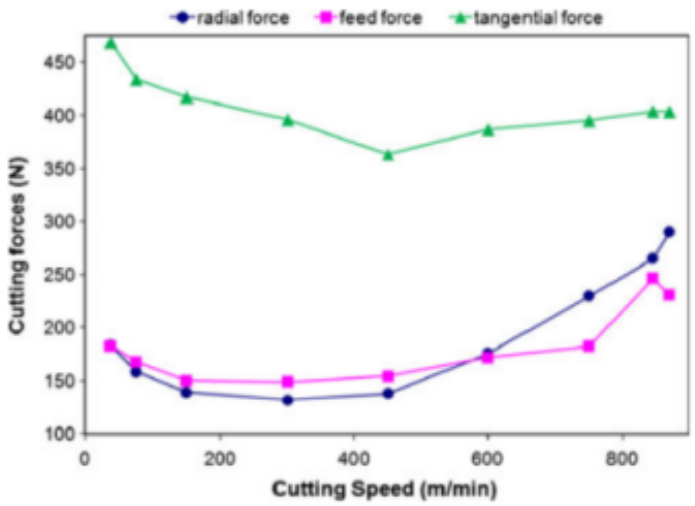

Figure 1.1: Evolution of cutting forces with cutting speed.
[26]

The specific cutting energy (SCE) is a function of cutting power and MRR being strongly influenced by cutting parameters. The higher the MRR for the same cutting power, the better the power consumption for cutting, which means the lower SCE [34]. Mativenga et al. [35] presented that by selecting cutting conditions such as feed rate, cutting speed and depth of cut in turning process, the reduction in energy foot print is about 64% compared to using recommended cutting data from tool suppliers. Silva et

al. [36] evaluated that the cutting forces increase drastically with the increase in feed rates, while the shear stress tends to reduce as feed rate is elevated during machining of AISI 1045 steel. Additionally, they found that the shear angle decreases and chip deformation increases as the chip compression ratio is elevated as shown in Fig. 1.2. Mori et al. [37] verified that in drilling process, the power consumption is decreased by increasing the feed rate and cutting speed within a value range which does not compromise the tool life. Yoon et al. [38] identified the energy consumption and manufacturing cost behavior in terms of the process parameters in drilling. They found that fast machining process can reduce the energy consumption because of decreased process time and only 35% of manufacturing cost can be saved. Hamade et al. [39] highlighted the benefits and challenges associated with drilling holes in aluminium by using aggressive combination of speeds and feeds in reducing the specific cutting power (and drilling forces) while removing substantial amount of material.

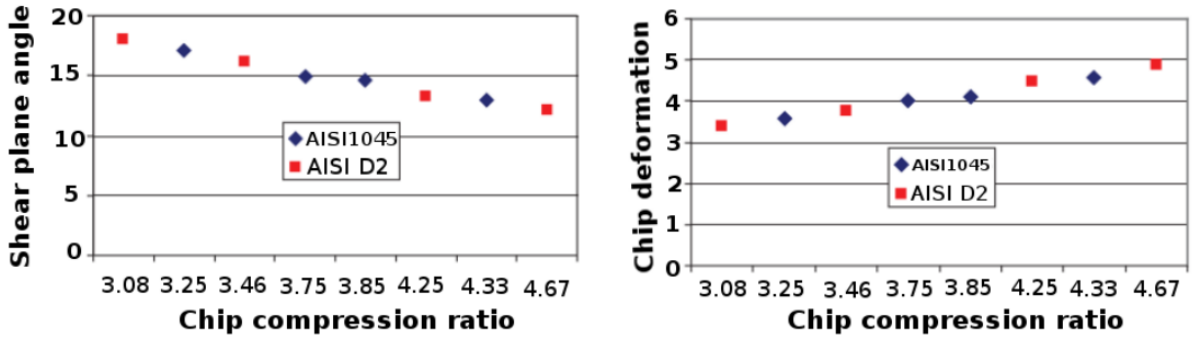

Figure 1.2: Experimental shear plane angle and chip deformation versus chip compression ratio.

[36]

Electropulsing as an instantaneous high energy input method, is recognized as one of the most important techniques in improving the machinability of material by reducing cutting resistance in metal cutting processes. The electrons exert a push on dislocations which is named as electron wind force. The electron wind force reduces the dislocation density and enhances the mobility of dislocation. In addition, higher current density pulses also increase the mobility of atoms and reduce the strength of the obstacles opposing dislocation [4]. Electroplasticity has demonstrated that it can improve the mechanical properties of material. Hui et al. [20] showed that electoplasticity can increase the strength and maintain the required high ductility by increasing the elongation of material. The effect of high density EPT not only heals the primary defects but also decreases the yield stress and yield to tensile ratio. The decrease in yield stress and yield to tensile ratio is helpful for increasing the formability and decreasing the spring-back to control the dimensional accuracy of sheet metal parts as shown in Fig. 1.3 [9].

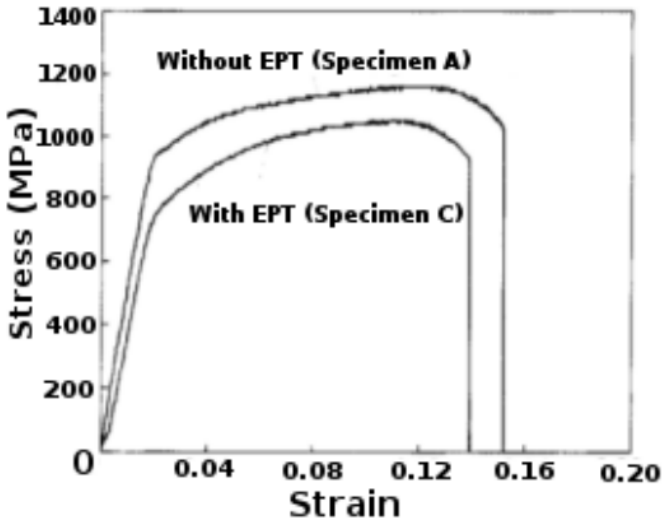

Figure 1.3: True stress-true strain curves of specimens A, B and C. [9]

Zhang et al. [40] found that the ultimate tensile strength was decreased and elongation ratio was increased with the application of EPs. Since, the yield stress and ultimate tensile strength have been decreased due to EPT which could be the reason why SCE has been decreased. Zhang et al. [41] also proved that cutting forces and hardness decreased and surface roughness improved in turning of specimens previously assisted by EPs of different frequencies as shown in Fig. 1.4.

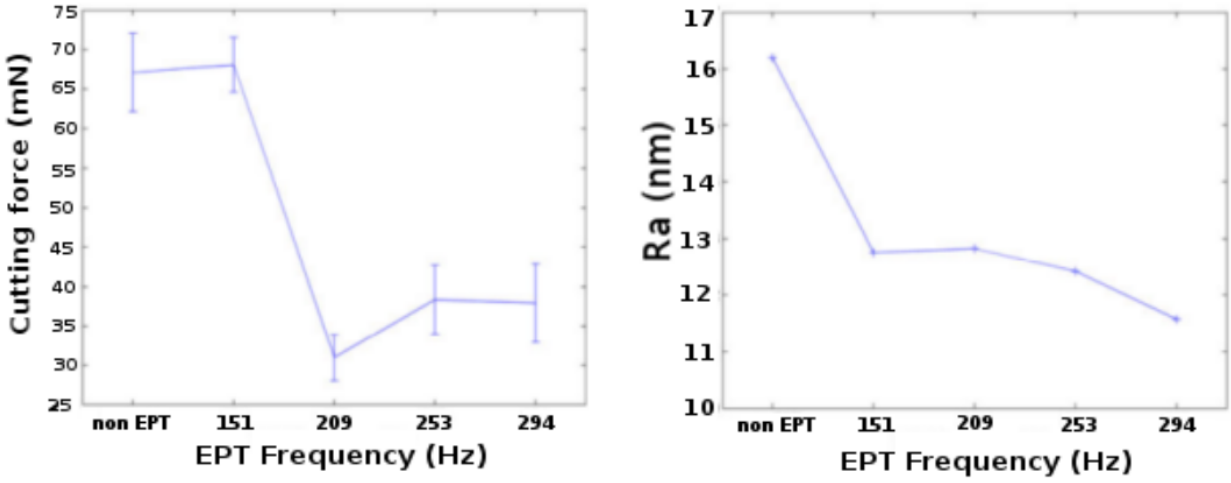

Figure 1.4: cutting force and Surface roughness under different frequency of EPT. [41]

Recently, Baranov et al. [42] have discovered that the effect of pulse current on

metal cutting area reduces the static force of cutting and hence the plastic deformation of metals. Sanchez et al. [43] stated that the power consumption and the SCE are decreased when the turning process is assisted with EPs as shown in Fig. 1.5. Also they showed that surface roughness can be improved while hardness decreased with EPs.

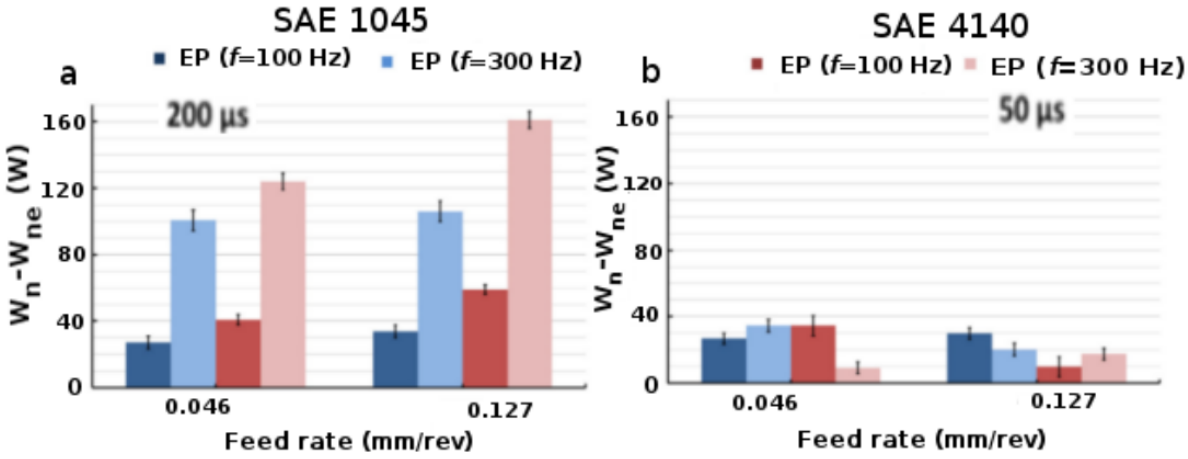

Figure 1.5: cutting force and Surface roughness under different frequency of EPT. [43]

The Fig. 1.5 showed the reduction in power consumed which is the difference between the net active power of conventional turning process and the net power of a EPs assisted turning process ($W_n - W_{ne}$). They performed the experiments with 200 μs pulses, 100 and 300 Hz frequencies for SAE 1045 and 4140 steel. They found that the assisted turning process is more efficient than the conventional turning, especially when higher values of frequency and greater pulse durations are induced. However, the energy saved dramatically decreases when the combination of higher values of frequency and shorter pulse duration are used.

Electroplastic effect in microstructure evolution

In material removal process, the chip undergoes severe plastic deformation under high strain rate and temperature. Pu et al. [44] experimentally observed the chip morphology as a function of cutting speed in AISI 1045 steel based on the criteria of minimum total energy consumed in the primary and secondary shear zone. They analyzed that when the cutting speed is increased, there is an onset of severe plastic deformation in the secondary shear zone and onset of microstructural softening event occurs as the temperature exceeds the critical values for dynamic recrystallization or phase transformation. At very high temperatures and low strain rates, dislocation density increases and grain growth becomes predominant to get fine grains, where complete dynamic recrystallization took place [45]. Sun et al. [46] observed the microstructure

evolution in cutting chips at different cutting speeds during machining and investigated that the morphology of chip changes from continuous chip to regular and irregular chip segments by increasing cutting speed. Also, the deformation twinning was observed inside the segment which is responsible for hardening inside the segment.

Hui et al. [21] examined that electroplasticity can be considered as an efficient method to refine grains by means of phase transformation and recrystallization in specimens of as-cast TiAl alloy and cold-rolled TA15 sheet when treated by high density electropulsing. The optical microstructues of the TA15 before and after treatment are shown in Fig.1.6. It is shown that recrstallization occurs in the sheets after EPT. The crystallized grains are very fine and uniformly distributed at lower temperatures compared with conventional heat treatment. Xu et al. [14] investigated that EPs accelerated the dynamic recrystallization at relatively low temperature and high strain rates due to two effects: the accumulation effect induced by the electron wind force which accumulates dislocations and leads to the formation of coarse grain boundaries and the annihilation effect induced by the coupling of thermal and electromigration effects annihilates dislocations and leads to the rearrangement of dislocation structures.

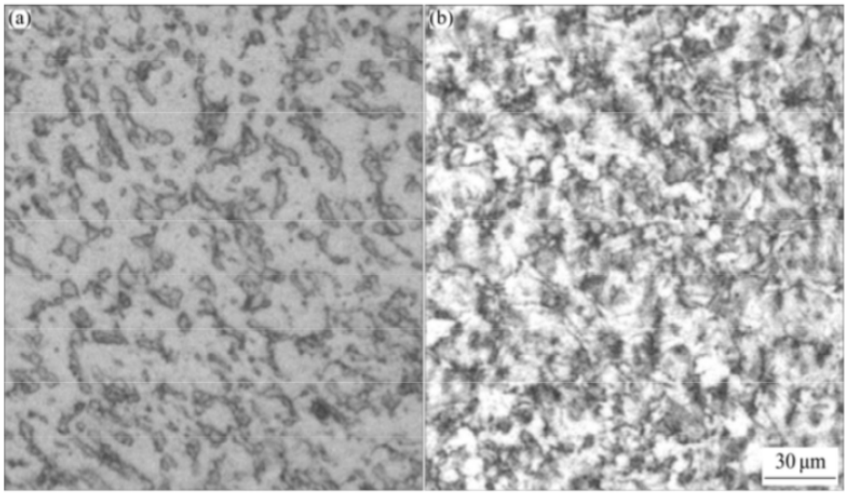

Figure 1.6: Optical microstructures of TA15 sheets: (a) Cold-rolled sheet; (b) Electropulsed sheet.

[21]

Zhang et al. [47] mentioned that various kinds of defects, such as large amounts of dislocation tangles and lattice distortions with many dislocation arrays and nodes were introduced from previously cold working process in the original samples as shown in Fig. 1.7a. After the EPT, most of dislocation arrays became straight and relatively stable state with less dislocation nodes was achieved as shown in Fig. 1.7b

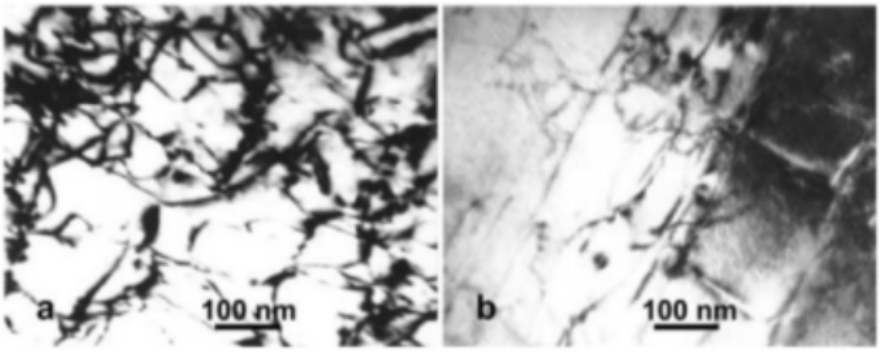

Figure 1.7: (a) The typical TEM images of the original samples and (b) the samples after electropulsing

[47]

Jiang et al. [19] studied the influence of EPs on microstructure of cold rolled AZ91 Mg alloy strips and examined that fine microstructure of quasi-single-phase-recrystallized grains can be obtained at relatively low temperature. The fracture characteristics of cold rolled AZ91 specimens are shown in Fig.1.8.

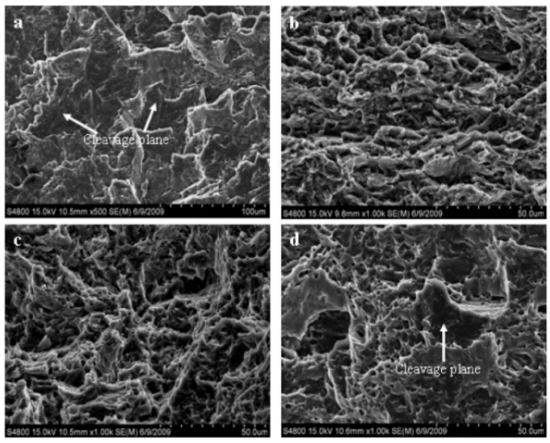

Figure 1.8: SEM fractographs of the samples after EPT: (a) cold-rolled sample, (b) 100 Hz-EPT sample, (c) 110 Hz-EPT sample and (d) 133 Hz-EPT sample..

[19]

When the frequency of EPT was increased to 110 Hz, the ductile fracture was observed with numerous dimples and tear ridges. By increasing the frequency to 133 Hz, some cleavage planes known as quasi-cleavage were found on fracture surface. Hence, recrystallization increased because of increase of EPT and the intensity of the basal texture of sample decreased gradually until recrystallization completed. They proposed that EPT subsequently increases the nucleation rate of recrystallization and atomic

diffusion due to the coupling of the thermal and athermal effects.

Zhang et al. [41] determined that with increasing frequency of electropulsing, both twins and dislocation density were reduced and decomposition and precipitation of β phase were tremendously accelerated in the AZ91 alloy. The optical micrographs of non EPT specimens and the EPT specimens with various frequencies of EPs are shown in Fig. 1.9. Many deformation twins were observed inside the grains of the cold rolled specimens of AZ91 alloy in Fig. 1.9 (a) without EPT and grain size was approximately 77 μm. When the frequency of electropulsing increased, the grain size and number of twins decreased. The average grain size reduced to 68 μm, 63 μm and 35 μm with frequencies of 209 Hz, 253 Hz and 294 Hz respectively in EPT specimens. A relatively homogeneous microstructure of equiaxed grains was observed at frequency of 294 Hz which implied that the EPs of high frequencies greatly accelerated recrystallization of specimens.

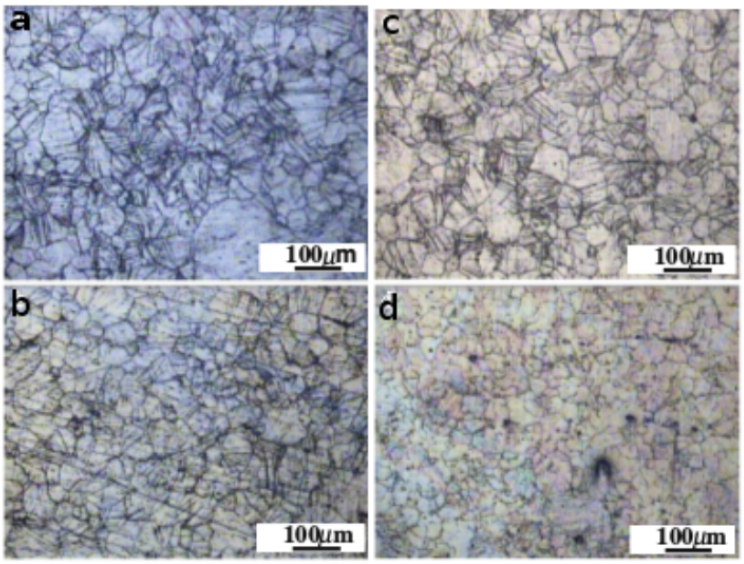

Figure 1.9: Optical micrographs of (a) non-EPT, (b) 209Hz-EPT, (c) 253Hz-EPT, and (d) 294Hz-EPT

[41]

All these studies have reported that the resistance to plastic deformation decreases significantly by EPT. They also indicated that the drift electrons help dislocations to overcome the resistance from obstacles, thereby resulting in a load drop. The experiments verified that yield strength, utlimate tensile strength, ductility, surface roughness, resistivity and elongation depend on the type of material and current intensity flowing through the material. Most of the studies are in agreement that mechanical properties and phase transformation occur due to the coupling of thermal and athermal effects. However, athermal effects on these properties remain under investigation.

Challenges of electroplastic manufacturing processes

There are various challenges that are still ahead before the successful application of electroplastic manufacturing processes. Some are listed below:

Development of electropulsing mechanism:
During electropulsing treatment, the thermal and athermal effects arising from EPs facilitate the manufacturing process. It is important to note that the values of thermal and athermal effects need to clarify the real reason for electroplastic effect and provide a theoretical knowledge to use electrical energy more efficiently.

Exploitation of new manufacturing processes:
More experimental and theoretical studies are required pertaining to manufacturing processes such as electroplastic deformation in drilling, turning and milling processes. These are important for the continuous sustainability of the technology. Although the progress of electroplastic manufacturing processes has been made in the past few years to understand the mechanism of electropulsing, further it needs to know how to pass large EPs to the deformation zone. The power sources are required to increase the process efficiency, unless the manufacturing cost should be controlled.

The main objectives of this research are listed in the following section.

1.1 Objectives

The main objective of this research work is to study the phenomenon of electroplasticity in various metal cutting processes. The constant current pulses of short duration are induced in the cutting zone with minimum possible plastic deformation that could improve the machinability of materials. The metal cutting processes studied are: drilling process and round turning process. All of theses processes are electrically assisted with short pulse duration and the results obtained then compared with conventional processes to study the machinability difference. To accomplish the main goal, it is proposed to set the following specific objectives.

- Design and develop the generator of short duration EPs to discharge multiple positive pulses and minimize the thermal effects (Joule effect) during machining processes.

- Electrically isolate the tool from the workpiece for each machining process during experiments for safety considerations.

- The electronic Watt meter was designed and developed to measure the nominal power consumption during each cutting process.
- Study the differences are presented in the conventional drilling process when compared with EPs assisted drilling process. The aim here is to analyze the variations of power consumption, SCE, chip compression ratio ξ, shear plane angle ϕ and thermal compressive stresses for conventional and assisted processes.
- Examine the variations of SCE, chip compression ratio ξ, shear plane angle ϕ and effect of high current densities for different materials during conventional and EPs assisted round turning processes.

1.2 Scope

Since, the main of research presented in the thesis is to improve the machinability of conventional metal cutting processes by using effect of current pulses, the scope of the study to accomplish different activities throughout research work is as follows:

a. The EP generator used to assist conventional cutting processes provide maximum current intensity of 140 A, frequency ranges from 100 to 300 Hz and duration of current pulses from 50 to 250 μsec.

b. Design and manufacture the electric Watt meter to record the power consumption during machining operation.

c. Design and manufacture electrical isolation system and electrical connectors to connect the workpiece and ctting tool with EP generatore for each cutting process.

d. The electrical parameters like frequency discharge and duration of short pulses are monitored by oscilloscope and frequency meter.

e. The mechanical power of motor for particular process is measured at different loading conditions to estimate the effective cutting power.

f. The machinability of material will be analyzed by using different mechanical parameters when the cutting process is assisted with current pulses compared with conventional process. The parameters analyzed for each process are:

- Cutting power consumption
- Specific cutting energy, SCE
- Thermal stresses
- Chip compression ratio ξ
- Shear plane angle ϕ

1.3 Thesis organization

1. Chapter 2: This chapter reported the effect of EPs in drilling process. The influence of EPs has been investigated on cutting power consumption, SCE, chip compression ratio ξ, shear plane angle ϕ and thermal stresses. The results are then compared with conventional drilling process to study the machinability differences for different materials.

2. Chapter 3: In this chapter, the machinability of materials has been studied by comparing the conventional turning process with electrically assisted turning process. The impact of high current density has been investigated on SCE, chip thickness, chip compression ratio ξ and shear plane angle ϕ and compared with conventional turning process.

3. Chapter 4: In this chapter, the general discussion is carried out about the results and limitations presented in the thesis.

4. Chapter 5: This chapter explains the main conclusions of the thesis and the recommendations suggested for future work that could be achieved in the following years.

1.4 Article Authorship and conference

Chapter 2 has been published in International Journal of Advanced Manufacturing Technology in Feb 2016. The article composition was done by Saqib Hameed. The Experimental procedure was performed by Sqib Hameed, Dr. Antonio Sánchez and Amelia Napolez. The current pulse generator and electric Watt meter were designed and manufactured by Dr. Hernán Alberto González Rojas. The article was reviewed for publication by Dr. Hernán Alberto González Rojas and Dr. Antonio Sánchez. (http://dx.doi.org/10.1007/s00170-016-8562-z)

Conference:

"An influence of electropulses on power consumption during drilling process" IMECE2016-65328, ASME 2016 International Mechanical Engineering Congress and Exposition, November 11-17, 2016, Phoenix, Arizona, USA

Chapter 2

Electroplastic cutting effect in drilling process

The aim of the present study is to report the use of non conventional material removal during metal cutting process. When the electropulses (EPs) are applied to metals undergoing plastic deformation, the deformation resistance reduces dramatically and plasticity increases at the same time. This influence of EPs on the plastic flow is called the electroplastic effect. Traditional metal cutting processes such as turning, drilling and milling rely mainly on the use of heat associated with cutting parts, which presents the largest expenditure of energy. Chip formation during machining is greatly influenced by cutting speed, feed rate and tool geometry. Selecting properly these parameters for a particular machining operation is very important to reduce tool wear and breakage as well as to achieve high machining efficiency. Speeds and feeds that are too high or too low, can reduce the efficiency of the whole operation [28]. In machining, optimum tool performance is achieved by selecting optimum cutting speed, feed, tool geometry and tool material depending upon workpiece material and quality requirements of machined surface.

Energy saving is considered as one of the most important factors in manufacturing industry. In drilling process, elevated shear stress induced by the cutting tool in the chip formation zone should exceed the strength of the work material. The distribution of these stresses must be such that the work material shows the strain at fracture as small as possible [27]. Geometrically, the surface is seen to have large number of minute irregularities (peaks and valleys) lead to stress concentration, which in turn induces residual stresses that influence the fatigue strength of critical parts besides causing harmful deformation. Therefore, surface quality is very important and its proper evaluation is of utmost interest as described by Astakhov [28]. Moreover, the main objective of machining is to separate a certain layer from the workpiece with minimum possible plastic deformation and thus energy consumption [27]. Therefore, energy spent on plastic deformation in drilling must be considered as wasted and EPs assisted drilling process is a novel technique that could reduce the power consumption.

In this research, a micropuls generator was used to assist the drilling process. A constant current intensity was induced in the cutting zone with a minimum possible plastic deformation that could improve the plasticity of material during the drilling process. The impact of EPs are analyzed on the power consumption, specific cutting energy, SCE and thermal stresses for different metallic materials. The ultimate objective is to study if differences are presented in the conventional drilling process when compared with the EPs assisted drilling process.

2.1 Methodology

An aeronautical aluminium alloy and a commercial steel alloy were chosen as workpiece materials for test samples. The specimens of aluminium alloy were cylindrical bars with a length of 20 mm and a diameter of 25 mm. Whereas the dimensions of steel alloy samples were 80 mm x 40 mm x 15 mm. The chemical composition of metallic materials is shown in Table 2.1.

Table 2.1: Material chemical composition.

7075 aluminium T6	% Al	% Zn	% Mg	% Cu	% Fe	% Si	% Mn	% Cr	% Zr
	87.2	6.1	2.9	2.0	0.5	0.4	0.3	0.28	0.25
1045 carbon steel	% C	% Ni	% Mo	% Cu	% S	% Si	% Mn	% Cr	% P
	0.45	0.17	0.05	0.35	0.035	0.26	0.60	0.10	0.02

Drilling process was carried out by using Huvema HU Profi Popular drilling machine. The tool was held by a standard tool holder. The cutting tool used was twist drill of high speed steel (HSS) with point angle of range 116^0-120^0 and helix angle of 20^0-30^0. The drill diameters were 3 mm and 4.5 mm. The polymer material was used to electrically isolate the workpiece and tool from drilling.

In drilling, the parameters used are spindle speed of 1050 rpm and a range of feed velocity is from 0.2 to 0.4 mm/s. The nominal power consumption was continuously measured by a self made monophasic energy analyzer linked to the motor of the machine. The sampling rate was analogic with storage after every 0.5 s. A self made short duration electric pulse generator was developed to discharge multiple positive pulses. The parameters of current pulses such as voltage, frequency and pulse duration were monitored by an oscilloscope, as listed in Table 2.2.

A schematic illustration of electrically assisted drilling process is shown in Fig. 2.1.

Table 2.2: Electropulsing operation parameters.

Material	Current intensity (A)	Pulse duration (μs)	Frequency (Hz)	Average output power (Watts)
7075 Al. 1045 Steel	140	250	300	300

The workpieces were cut by facing process to make sure the surface was smooth. The carbon clamps were attached on one side with round smooth element in the tool holder and on other side connected with generator through wire. The workpiece was also connected with generator through wire. Then, drilling operation was performed without EPs (conventional process). Subsequently, the same procedure was performed but assisted with EPs. The EPs were induced when the drill was already in contact with the material, in order to avoid sparking (electroerosion). Later, the power consumption and SCE of both processes have been compared. Finally, the removed chip was thoroughly polished and prepared to measure the chip thickness with an optical microscope.

2.2 Results and Discussions

2.2.1 Current density and cutting configuration

In a material removal process the large strains are imparted to the chip at the primary deformation zone [48]. For this reason it is necessary to estimate the current density induced in this zone. The current density is defined as current intensity which goes through the cross-sectional area of the material. Here it is assumed that the current flows through the tool-chip contact length and then goes across the shear cutting area, making a close electric circuit with the workpiece. The shear cutting area is defined by the segment OA and the length of the cutting edge b, as shown in Fig. 2.2.

The nominal chip thickness or undeformed chip thickness a can be estimated as:

$$a = \frac{f}{2} \cdot sin(\frac{\varphi}{2}), \tag{2.1}$$

where f is the feed rate (mm per second), φ is the point angle (°).

Additionally, the segment OA is described by:

$$OA = \frac{a}{sin(\phi)}, \tag{2.2}$$

where ϕ is the shear plane angle (°).

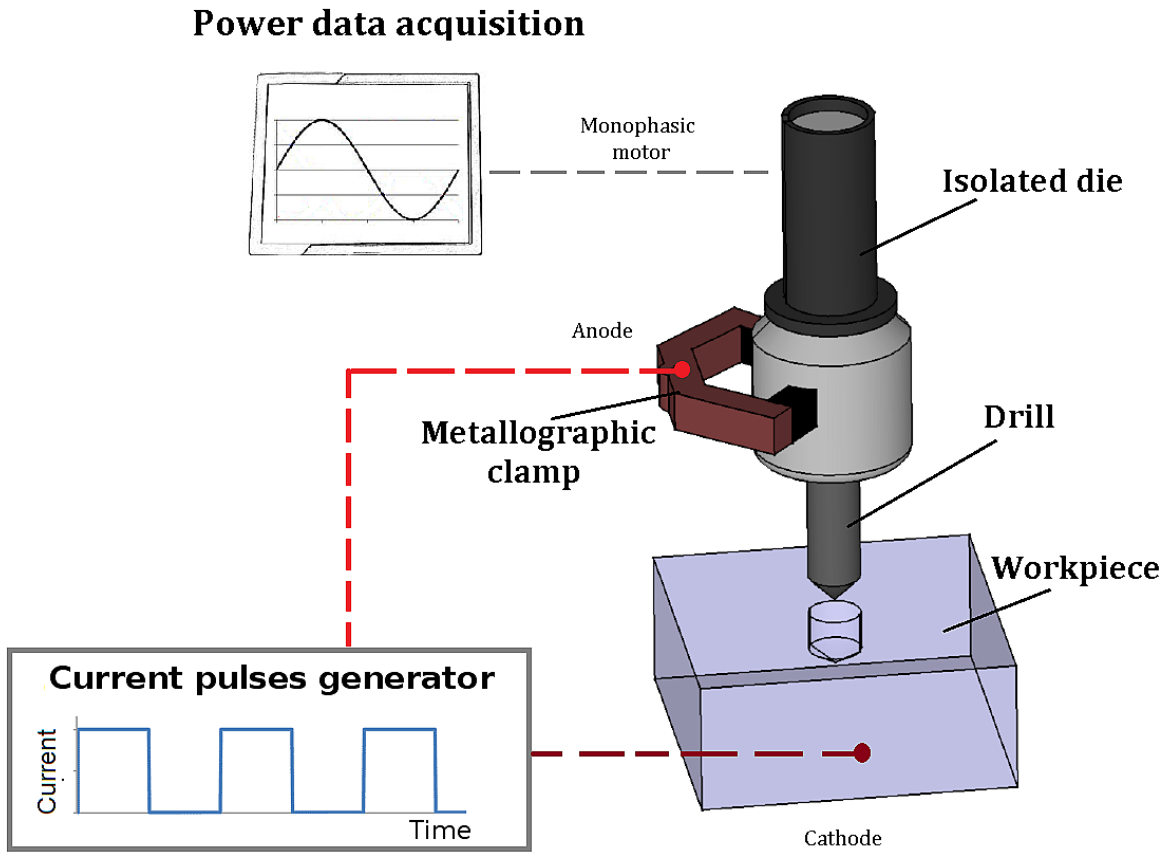

Figure 2.1: Schematic of electrically assisted drilling process.

Then, the nominal cutting width is defined by:

$$b = \frac{\frac{0.85 \cdot d_r}{2}}{sin(\frac{\phi}{2})}, \tag{2.3}$$

where d_r is drill diameter (mm).

Consider the shear angle plane of drill bit to estimate the current density J_e at cutting edge of drill. Therefore, the current density can be calculated by the following equation

$$J_e = \frac{2 \cdot I \cdot \sin(\phi)}{0.8 \cdot f \cdot d_r}, \tag{2.4}$$

where I is the current intensity (A).

The shear plane angle ϕ proposed in [49] can be expressed geometrically by chip compression ratio ξ as

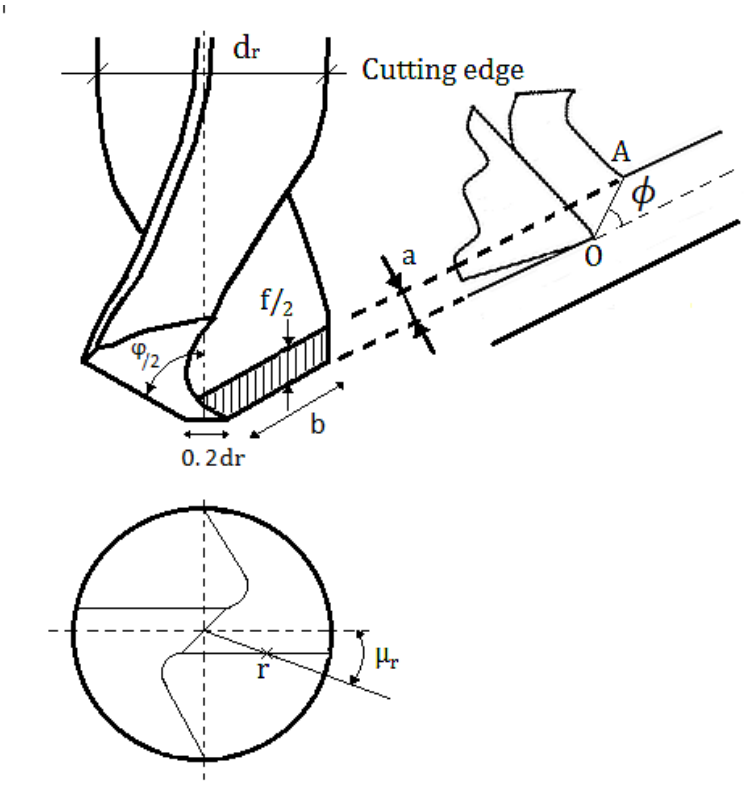

Figure 2.2: Graphical model for the determination of uncut chip thickness.

$$\phi = \arctan\left(\frac{\cos\alpha}{\xi - \sin\alpha}\right). \tag{2.5}$$

Chip thickness coefficient defined as a ratio $\xi = a_1/a$, where a_1 is deformed chip thickness. α is the rake angle which is also helix angle in drilling. The value of helix angle for drills under study is 30°.

The chip removed by the drilling tool was encapsulated in resin. A conventional polishing process was conducted until revealed the cross sectional area presented in Fig. 2.3 (a). The average chip thickness was measured by capturing the images with an optical microscope to calculate the area and the length of the chip in pixel and then convert into mm with a calliper. The average chip thickness is defined as the quotient between the cross sectional area of the chip and the chip length. Each value of chip thickness is the average of ten measurements and the margin error is up to 8% of a standard deviation estimation. The Fig. 2.3 (b) exhibits the zoom of the cross section of chip used to calculate the chip thickness experimentally.

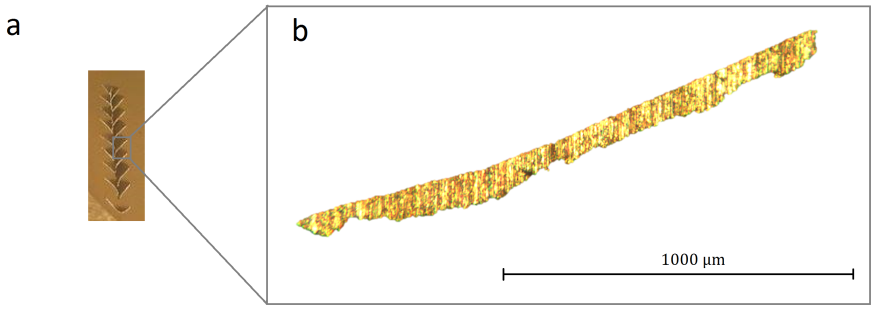

Figure 2.3: (a) Cross sectional area of chip. (b) Zoom of a single chip segment.

The drill used during the experiments has not automatic feed rate configuration; therefore it was necessary to estimate the feed velocity and the spindle velocity to be able to calculate the feed rate f. An optical ON/OFF switch control with a timer was used to measure the feed velocity. A metallic strip attached to the axle of the drill was used to change the switch status. Subsequently, the feed velocity was defined by the strip length and the time registered with the timer. The spindle velocity in rpm was measured with a conventional tachometer. Table 2.3 gives the values of chip compression ratio, shear plane angle and current density as a function of feed rate in drilling for 1045 carbon steel and 7075 aluminium.

Table 2.3: Values of chip compression ratio ξ, shear plane angle ϕ and current densities as functions of feed rates.

Material	Drill dia (d_r) [mm]	Feed rates (f) [μm/rev]	Undeformed chip thickness (a) [μm]	Chip compression ratio (ξ)	Shear angle (ϕ) [°]	Current density (J_e) [A/mm^2]
7075 Al.	3	97.71	41.52	3.37	16.79	354
	4.5	18.68	7.93	5.33	10.15	758
1045 Steel	3	48.17	20.47	4.37	12.61	544
	4.5	51	21.67	4.53	12.12	329

It can be noticed that the shear angle ϕ decreases as the chip compression ratio ξ increases. Also, the chip compression ratio ξ decreases with the increase of feed rate. The chip compression ratio ξ can be considered as a measure of plastic deformation of material [28]. The high values of chip compression ratio (low ϕ values) mean large amount of strain in the shear plane. The results of chip compression ratio obtained were comparable with those evaluated by Silva et al. [36] to study the machinability of 1045 carbon steel. By comparing the operating parameters with the present work, it

was observed that the difference in results was about 3%. Therefore, the values of chip compression ratio and shear plane angle give an intensive amount of plastic deformation at the shear zone. The current density increases with the decrease of feed rates during electrically assisted drilling process as shown in Table 2.3. The effect of these densities is presented in the section of thermal expansion to calculate the adiabatic temperature rise and thermal stresses in the materials.

2.2.2 Thermal expansion

The high rise of temperature described by Joule heating effect is calculated to determine the contribution of factor in the electrically assisted drilling process. Okazaki et al. [6] observed that the thermal effect of electropulsing can reduce the deformation resistance and improve the plasticity of material. They described the adiabatic rise of temperature, ΔT for a single EP by the following equation;

$$\Delta T = \frac{J_e^2 \cdot \rho \cdot t_p \cdot f}{C_p \cdot D}, \tag{2.6}$$

where J_e is the effective current density, also called root mean square value of current density, ρ is the resistivity, t_p is the EP duration, f is the frequency discharge, C_p is the specific heat and D is the density of materials.

Table 2.4: Properties of materials.

Material	ρ (Ωm)	C_p (J/Kg°C)	E (GPa)	α ($^{\circ}C^{-1}$)	D (Kg/m^3)
7075 Al.	5.15×10^{-8}	960	71.7	21.6×10^{-6}	2810
1045 Steel	1.62×10^{-7}	486	206	11.5×10^{-6}	7850

To calculate the adiabatic rise of temperature, the properties of materials are shown in Table 2.4. An adequate thermal effect resulting from the Joule heating effect of electroplastic treatment is necessary to increase the nucleation rate of recrystallization [8]. The exact mechanism of athermal effect is still not very clear; however, there is possibility that it results from additional force of electrons exert on dislocations called electron wind, the Joule heating effect and thermal stresses. Due to very short duration, the tremendous force should be impacted which further enhances irregular speed of atoms based on thermal effect. As the electron wind force increases, the higher athermal effects will be induced due to higher values of electron current density [13]. The defects such as micro-crack, cavity and void can be produced in machining processes. Because of these defects, the resistivity is higher in the area with defects than that without defects. When the EPs are passed through the metal specimen, the temperature rise

is higher in the area with defects than that without defects due to inhomogeneous resistivity in the metal. This inhomogeneous rise of temperature causes inhomogeneous thermal expansion and the defected area suffers compressive stresses as compared to area without defects [35].

Then, based on the high-rate heating of EPs, the maximum thermal stress suggested by Tang et al. [11] can be written as:

$$\sigma_{max} = E \cdot \alpha \cdot \Delta T, \tag{2.7}$$

where E is Young's modulus and α is the coefficient of thermal expansion.

Table 2.5: Adiabatic temperature and thermal stress values.

Material	Drill diameter (mm)	ΔT (°C)	σ_{max} (GPa)
7075 Al.	3	179	0.28
	4.5	823	1.27
1045 Steel	3	942	2.23
	4.5	345	0.82

When the current pulses of short duration passed through the specimen, the Joule heating effect occurred in the specimen. Due to very short duration of EPs, the material particles undergo heavy stress impact [10]. Because of the increase of current density, a higher rise in temperature would be produced and hence the maximum stresses will be increased during EPs treatment, as shown in Table 2.5. Then, higher thermal stresses would be induced by increasing the current density, which is strong enough to accelerate the motion of dislocations [5]. Accordingly, nucleation rate of recrystallization can be increased by advancing the mobility of dislocations during EPs treatment [50]. Hence, electrically assisted processes play a vital role in the modifications of mechanical properties of materials.

2.2.3 Power consumption

Energy consumption in machining processes is one of the key parameters that plays an important role during cutting and is a function of cutting speeds, feed rates and workpiece material [27]. Stephenson et al. [51] defined that the specific cutting power also called SCE is the amount of energy spent to cut per volume of the work material per unit time. It is often used to compare the machinability of different materials, especially when relative tool life data are unavailable. Ekincioglu et al. [52] stated that

efficient cutting process requires maximum cutting speed and minimum SCE. Therefore, the SCE becomes a measure of cutting efficiency and a criterion as well. The SCE is the sum of the energy consumed in the primary, secondary and tertiary deformation zones [53].

The power consumption during the cutting process was measured by self made energy analyzer. The net active power W_n is determined by taking the difference between the average power when the cutting tool is removing the material and the power when machine is idle. In this section, the net power obtained in a conventional drilling process is compared with a power obtained in electrically assisted drilling process. The hypothesis is: the net power consumed in assisted drilling process is less than the power consumed by conventional drilling process.

Table 2.6: Specific cutting energy and power consumption.

Material	Drill diameter (d_r) (mm)	Feed rates (f) (μm/rev)	E_s (SCE) (W.s/mm^3)	N_c (W)
7075 Al.	3	12.91	7.55	12.03
(without EPs)	4.5	9.08	5.72	14.08
7075 Al.	3	11.94	5.49	8.05
(with EPs)	4.5	7.42	4.77	9.62
1045 Steel	3	21.94	4.16	11.29
(without EPs)	4.5	17.65	4.32	21.08
1045 Steel	3	22.45	3.94	10.96
(with EPs)	4.5	18.34	3.61	18.32

In Table 2.6 the values of SCE and power consumption as a function of feed rates are presented for 7075 aluminium and 1045 carbon steel with pulse duration of 250 μs, frequency of 300 Hz and drill diameters of 3 mm and 4.5 mm. All the values are the average of ten measurements registered in each case during conventional and assisted drilling processes. The margin errors represent the t-student distribution with a 95% confidence interval.

Figure 2.4 shows the reduction in SCE and power consumption due to the application of EPs during drilling process. The maximum reduction of SCE was observed 2.06 W s/mm^3 for 7075 aluminium and the least was observed 0.22 W s/mm^3 for 1045 steel with 3 mm drill diameter. Similarly, the maximum reduction of power consumption was noted 4.46 W for 7075 aluminium with drill diameter of 4.5 mm and the least was 0.33 W for 1045 steel with drill diameter of 3 mm. The use of pulses with high frequency and large duration values shows a large reduction of SCE and power

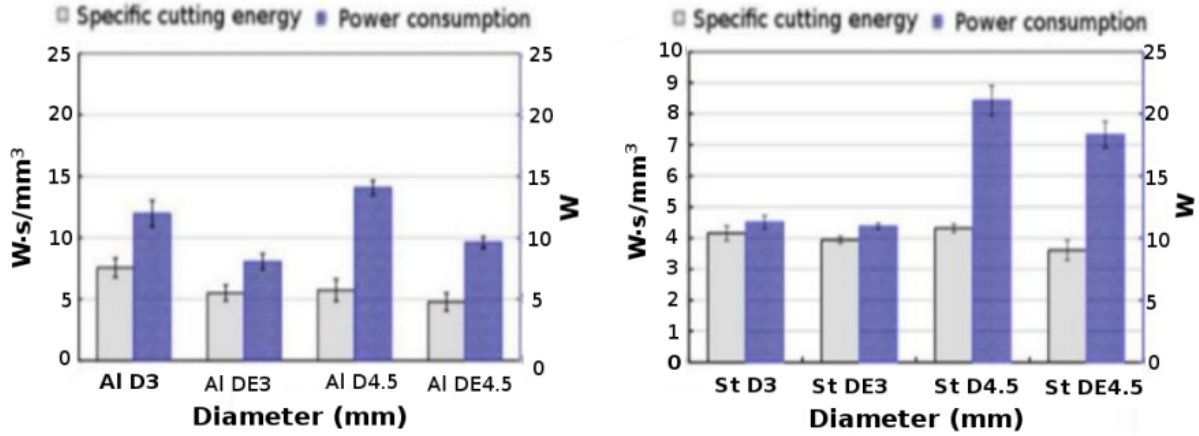

Figure 2.4: Specific cutting energy and power consumption for 7075 aluminium (a) and 1045 carbon steel (b).

consumption. These results show an improvement of the material machinability when drilling process is assisted with EPs compared with the conventional drilling process.

Sood et al. [54] stated that SCE can be calculated as quotient of the net energy and material removal rate. The material removal rate Q_c is the volume of material removed per unit time. In this particular case, it is estimated by a feed velocity which crosses perpendicularly to the section of the material removed by the drill. Therefore, the Q_c (measured in mm^3/s) is a function of cutting conditions and can be written as:

$$Q_c = \frac{\pi \cdot d_r^2}{4} \cdot V_f, \tag{2.8}$$

where V_f is feed velocity (mm/s) and d_r is the drill diameter.

Then, the SCE is the energy consumed per unit of volume of the material removed and can be described as,

$$E_s = \frac{N_c}{Q_c}, \tag{2.9}$$

where N_c (W) is the effective cutting power consumed during drilling.

The material's machinability during EP assisted drilling process was determined by comparing the SCE with respect to the conventional drilling process. To do that, the SCE was calculated by Eq. 2.9, where the power consumption and the material removal rates were measured experimentally, for both processes, conventional and assisted drilling process. The material removal rate was previously estimated with Eq. 2.8. This equation has been recalculated for each measurement because of the differences in feed rates between the conventional and the assisted drilling processes. To

compare the assisted process with the conventional process, the percentage of reduction r_p in the SCE is evaluated. This reduction is defined as:

$$r_p = 1 - \frac{E_s(assisted)}{E_s(conventional)}, \tag{2.10}$$

In Table 2.7, the percentage of SCE reduction values are presented for 7075 aluminium and 1045 steel, calculated from Eq. 2.10 for drill diameters of 3 mm and 4.5 mm, 300 Hz frequency and 250 μs pulse duration.

Table 2.7: Specific cutting energy percentage reduction

d_r (mm)	Frequency (Hz)	Duration (μs)	7075 Al. ($\%r_p$)	1045 Steel ($\%r_p$)
3	300	250	27.3	9.9
4.5			16.7	16.6

The results showed that the current pulses of high frequency and large duration gave a large decrease in SCE and cutting power consumption, N_c. The 7075 aluminium presented a SCE reduction of approximately 27.3 and 16% and reduction in N_c of about 33% and 31% with drill diameters of 3 mm and 4.5 mm respectively. Similarly 1045 carbon steel registered reduction of SCE of approximately 5.3 and 16.43% and reduction in N_c of about 3 and 13.1% with drill diameters of 3 mm and 4.5 mm respectively. Baranov et al. [39] discovered that plastic deformation of metals becomes easier by superimposing pulse current on metal cutting area in drilling process, which decreases the static force of cutting and increases the speed of cutting. Hence, due to the thermal contribution of EPs, the deformation resistance decreases [38], which ultimately decreases the SCE and N_c, so improves the plasticity of material during EP assisted drilling process. However, the results are also in agreement with Sánchez et al. [40], where the maximum reduction in SCE was 25% for EPs of 300 Hz frequency and 200 μs in turning process.

2.3 Conclusion

The influence of the electropulses in the cutting material have decreased the resistance of material to be plastically deformed, which ultimately reduces the specific cutting energy and improves the plasticity of material during EP assisted drilling process.

There is a correlation between chip compression ratio ξ , shear angle ϕ, feed rates, and current density in EPs assisted drilling process. When lower feed rates are used and subsequently, higher current density values are induced, the shear angle decreases

and the chip compression ratio increases.

The specific cutting energy is reduced up to 27% in 7075 aluminium and 17% in 1045 steel when the drilling process is assisted with EPs. The electrically assisted drilling process seems to have influence on improving the material machinability, but further investigations need to be done with different EPs configurations to determine the trends and contributions of each electrical parameter.

Chapter 3

Electroplastic cutting effect in the round turning process

Machining of metals and alloys plays a crucial role in the manufacturing industry, including the ultra precision machining of extremely delicate components [55]. Plastic deformation of the layer being removed in the form of chip is the greatest nuisance in metal cutting, i,e the energy required to remove the material as plastically deformed chip should be minimized to achieve high process efficiency [56]. The cutting speed influences the energy spent on the deformation of the chip through the temperature, dimensions of the deformation zone adjacent to the cutting edge and velocity of deformation. An increase in cutting speed leads to decrease of the plastic deformation in the chip formation zone and this region of plastic deformation becomes smaller because of increase of cutting speed [27]. Generally, in metal cutting processes, the reduction in energy spent in metal cutting is of great importance, as only 30-50% of energy is spent for useful work while 25-60% of energy consumed by cutting system is simply wasted [57]. Therefore, the prime objective of the cutting process is to reduce this energy to the lowest possible by selecting properly the tool material, machining regime and process parameters.

Since, the energy consumption in machining processes is one of the key parameters that plays a vital role during cutting and is a function of cutting speeds, feed rates and workpiece material [31]. In turning of medium carbon steel, the SCE, the amount of energy required for unit volume of material decreased when the feed and depth of cut are simultaneously high [58]. Adam et al. [59] evaluated the influence of feed rates and cutting speed on the thickness of chip being produced. They found that the chip thickness decreased as the cutting speed and feed rates decreased. Moreover, Gui et al. [60] studied the influences of uncut chip thickness on the cutting forces and SCE. They investigated that increasing the uncut chip thickness increases the cutting force while, SCE increases linearly when the uncut chip thickness decreases from 150 micron to 10 micron.

The physical phenomenon that govern the problem of material removal are complex. Many approaches have been proposed for quantifying the flow stresses of material at elevated strains and strain rates combined with temperatures during machining. Merchant [61] is the first to develop an orthogonal cutting plane based on the principle of minimum energy under the basic assumption that the deformation occurs in a single cutting plane, producing a single discontinuity in the velocity field. The hypothesis of a single cutting plane makes it difficult to include the effect of hardening by strain rate, which is known to be significant factor in high speed deformation processes. Examining Merchant's theory with respect to the prediction of cutting plane angle, Oxley [62] proposed a new model of shear stresses parallel sides, based on direct observation of chip formation. This model has many characteristics of the model developed by Merchant but it introduces as novelty of strain hardening ad temperature effects in the properties of material. Subsequently, Adibi-Sedeh et al. [63] extends the theory developed by Oxely to predict forces in different materials and Lalwani et al. [64] does so to predict temperature by using Johnson-Cook (J-C) model. They found that J-C model obtains better results in the prediction of forces amongst the different models studied. Taunsi et al. [65] estimates the coefficients of the constitutive equation of J-C used in the model of one dimensional cutting of two parts. Dudzinski y Molinari [66] developed a thermomechanical model of orthogonal cutting for high speed machining. Assuming that the hydrostatic pressure is constant in the primary shear zone and the equation of motion is reduced to a single relationship by calculating inertial force. All the aforementioned models of metal cutting considered plastic deformation as a quasi-static process, assuming that the inertial forces due to plastic flow are negligible.

Becze et al. [67] noted that the adiabatic temperature rise presented considerable heating of shear band in the specimen at elevated strain rates. They also indicated that the temperature rise in the shear band will decrease the flow stress of material due to constitutive laws. The plastic deformation starts when the material passes through primary deformation zone and is sheared at a rapidly increasing strain rates until the strain rate reaches its maximum value [68]. Lee et al. [69] studied the phenomenon associated with large strain deformation in the primary shear zone by using particle image velocimetry (PIV) technique. They examined that the shear strain rate increases linearly with the cutting speed and the shear zone is narrower for higher shear strain rates. Oxley et al. [70] determined that the plastic deformation zone is smaller for lower rate of strain hardening materials to give a reduction in cutting force with corresponding increase in chip thickness ratio ξ, that is the material is removed with less deformation. Higher strain rates and cutting speeds significantly reduce the energy required to accomplish the process [71]. Since the sensitivity of material deformation to micro defects increases with chip thickness, the energy required in removing unit volume of material decreases [72]. Bakkal et al. [73] investigated that machining at high cutting speed significantly reduces the SCE for material with low thermal conductivity and high thermal softening. The electrically assisted turning process can be considered

as a novel technique to reduce the plastic deformation in the deformation zone and thus the energy consumption by optimizing cutting conditions during machining.

In the following sections, an experimental methodology is succeeded with several experiments to record the electrical and mechanical parameters. A model of orthogonal cutting was also developed to study the strain, strain rate and temperature distributions in the primary deformation zone.

3.1 Experimental set up

The turning process was carried out by using WEISS WMP280V-F round turning machine. A tungsten carbide tool with a rake angle of 6° was used and held by standard tool holder to machine the metallic bars. The purpose of cutting edge angle is to relieve the cutting edge to prevent rubbing the machined surface. The commercial steel alloys (S235) and aluminium alloys (Al 6060) of 20 mm diameter were chosen as workpiece materials for test specimens. The chemical composition of metallic materials is shown in table 3.1 and mechanical properties of materials are shown in table 3.2

Table 3.1: Material chemical composition.

Al 6060	% Al	% Zn	% Mg	% Cu	% Fe	% Si	% Mn	% Cr
	97.9	0.15	0.35	1.0	0.1	0.3	0.10	0.05
Steel S235	% C	% N	% Cu	% S	% Mn	% Cr	% P	
	0.17	0.012	0.55	0.04	1.4	0.3	0.04	

Table 3.2: Mechanical properties of materials.

Material	ρ (Ωm)	C_p ($J/Kg°C$)	E (GPa)	α ($°C^{-1}$)	D (Kg/m^3)
Al 6060	3.2×10^{-8}	900	70	21.6×10^{-6}	2700
Steel S235	1.42×10^{-7}	450	210	12×10^{-6}	7900

A polymeric material was used to electrically isolate the workpiece and tool holder from the lathe. The machining parameters used are shown in table 3.3. The power consumed was continuously measured by a self made monophasic energy analyzer linked to the motor of the machine. A self made short duration electric pulse generator was developed to discharge multiple positive pulses. The parameters of current pulses such as voltage, frequency and pulse duration were monitored by an osciloscope as listed in table 3.4.

Table 3.3: Turning operation parameters.

Material	Spindle speed (rpm)	Feed rate (mm/rev)	Depth of cut (mm)
6060 Al. S235 Steel	600/900	0.07/0.14	0.2/0.4

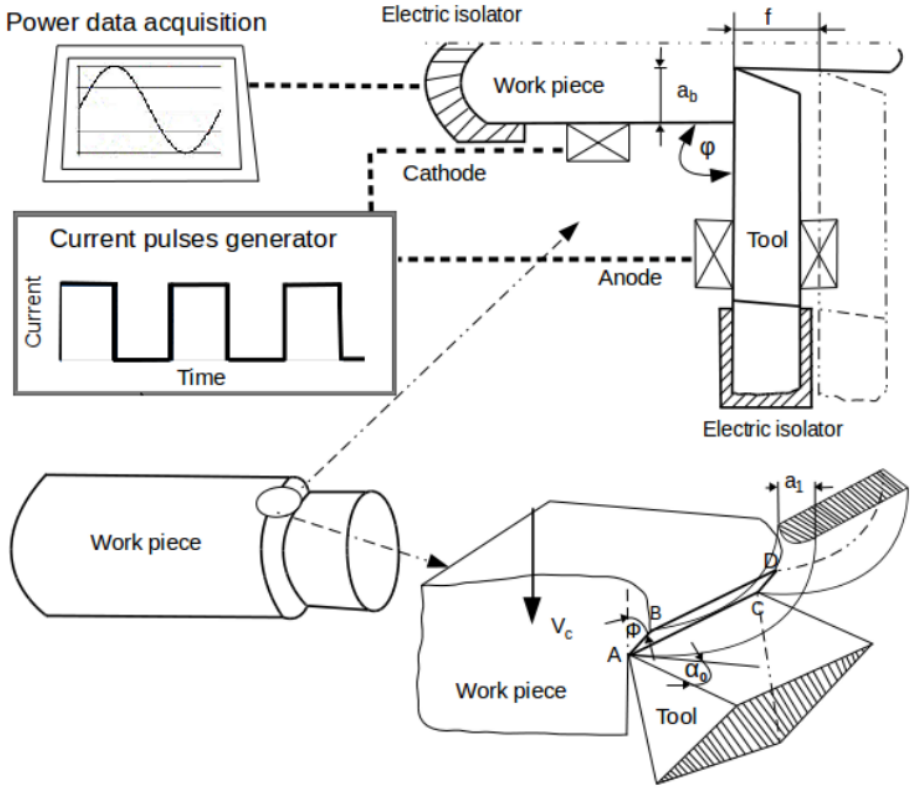

Figure 3.1: Schematic of electrically assisted turning process.

Table 3.4: Electropulsing operation parameters.

Material	Current intensity (A)	Pulse duration (μs)	Frequency (Hz)
6060 Al. S235 Steel	140	250	300

A schematic illustration of electrically assisted turning process is shown in Fig. 3.1. The workpieces were performed round turning process to make sure the surface was smooth and symmetric. The carbon clamps were attached with workpiece and connected on one side with cutting tool and on the other side with generator through wire. The turning operation was performed without EPs (conventional process). Subsequently, the same procedure was performed with EPs assisted process and made sure that the workpiece was already in contact with the tool to avoid electro-erosion.

3.2 Model of cutting zone

The metal cutting is considered to be taking place in a system consisting of tool, workpiece and the chip, through which the external energy applied causes the fracture of layer being removed [57]. Chip formation occurs due to concentrated shear within a narrow zone often called as primary deformation zone in the shear plane [69]. The process of orthogonal cutting of ductile material in finishing condition is shown in Fig. 3.2. Assuming a reference system with respect to material, the problem of chip removal is reduced to a stationary process, where the workpiece moves at a speed V_c downwards and chip leaves with speed V_{ch}. Assuming the Merchant hypothesis, the mechanism of chip removal is characterized by a shear stress on shear plane OA. A characteristic geometric parameter of chip removal processes is chip thickness ratio ξ, defined as the ratio between the chip thickness a_1 and chip thickness before cutting which in the case of cylinder advanced by turn f. Large value of ξ means more thickening at low feed rates i,e more effort is required in terms of forces or energy to accomplish the cutting process. Therefore, it is always desired to reduce ξ without sacrificing productivity.

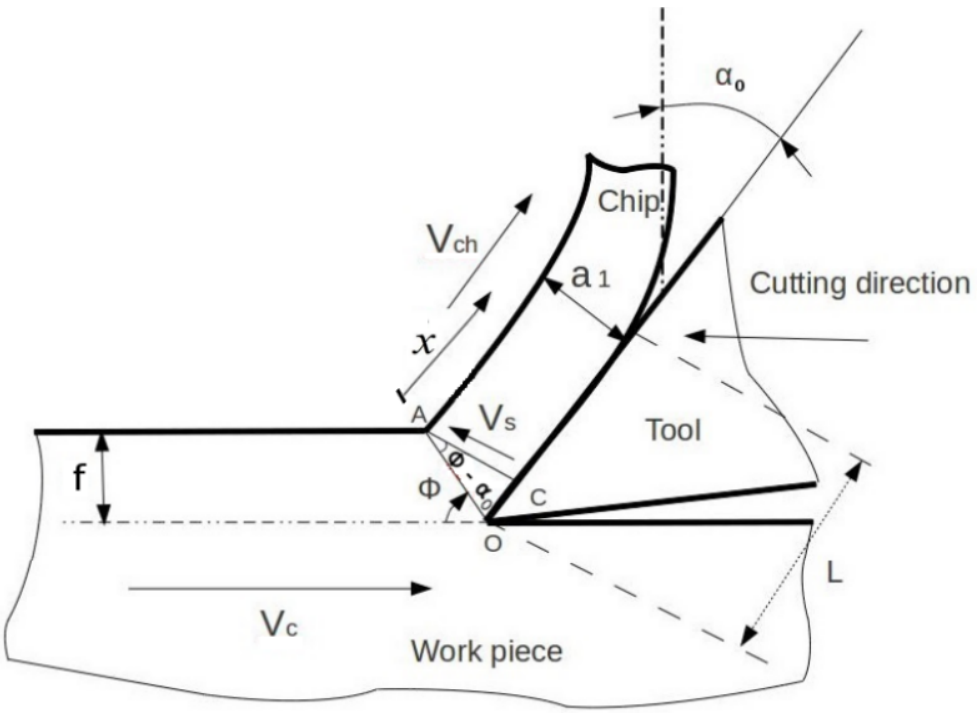

Figure 3.2: Orthogonal cutting plane.

From the geometry of orthogonal cutting, the known expression is derived to obtain shear plane angle ϕ.

$$tan(\phi) = \left(\frac{\cos \alpha_0}{\xi - \sin \alpha_0} \right). \tag{3.1}$$

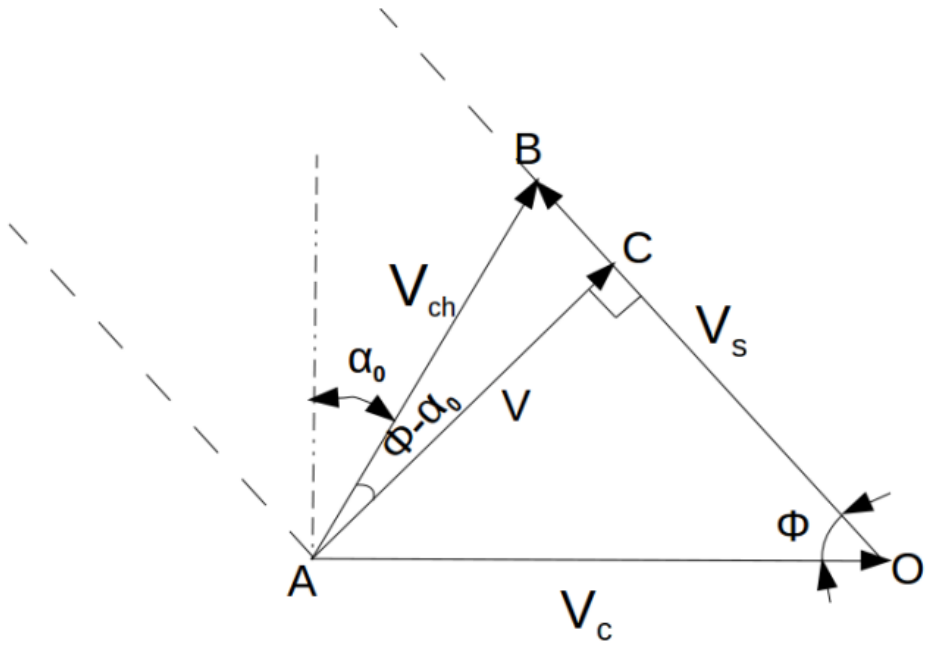

Figure 3.3: velocity diagram of orthogonal cutting.

where α_0 is the rake angle

The law of conservation of mass is applied to orthogonal cutting process in which the material flows in a continuous slip of cutting allows to obtain velocity of chip V_{ch}.

$$V_{ch} = \frac{f}{a_1} \cdot V_c \tag{3.2}$$

where V_c is the cutting velocity. f is the feed rate (mm/rev) which is also undeformed chip thickness.

The shear velocity in the shear zone is obtained from the velocity hodograph as shown in Fig. 3.3. This velocity is associated with energy dissipation that occurs in shear plane.

From the velocity diagram, the magnitude of velocity, V_s in the shear zone is given by

$$V_s = V_c \left(\frac{\cos \alpha_0}{\cos(\phi - \alpha_0)} \right). \tag{3.3}$$

The plastic shear strain γ can be estimated as quotient between the change in displacement experienced by shear plane ΔS and change in displacement from the normal direction to shear zone Δx

$$\gamma = \tan(\phi - \alpha_0) + \frac{1}{tan(\phi)} \tag{3.4}$$

Considering that the material flows when the effective stress at a given point in the material exceeds effective pure stress τ. The rate of energy dissipated along discontinuity is

$$\dot{W}_s = \tau \cdot V_s \cdot e \cdot \frac{f}{sin(\phi)} \tag{3.5}$$

where e is the thickness of the tube.

The heat transfer during orthogonal cutting is governed by one dimensional heat equation. In the cutting process the edges of cutting band are considered adiabatic [74]. Due to the velocity with which moves, the contribution of heat by diffusion is negligible compared to the convection heat flow. Likewise, the friction in the primary shear zone can be considered negligible. Therefore, the rate of heat generation per unit volume depends only on the plastic deformation. Assuming that the fraction β of plastic deformation is converted to heat. The equation of heat can be reduced to

$$\rho \cdot C_p \cdot u \frac{dT}{dx} = \beta \cdot \tau \cdot \dot{\gamma} + \dot{q} \tag{3.6}$$

where T is the temperature in the shear zone, ρ is the density of workpiece, C_p is specific heat, β is the coefficient of Taylor-Quinney when plasticity occurs, x is the direction normal to shear zone as listed in Fig. 3.2 and $\dot{q}$ is Joule heating effect which can be written as

$$\dot{q} = \frac{\rho_e \cdot h \cdot sin(\phi)}{e \cdot f} \cdot i^2 \tag{3.7}$$

where ρ_e is the resistivity of material, h is the thickness of primary deformation zone and i is the current intensity.

Moreover, the workpiece material is assumed to be homogeneous and isotropic and is governed by constitutive equation of Johnson-Cook (J-C). This model expresses the effective pure shear stress τ as a function of effective plastic strain, the effective strain rateand temperature. Currently the J-C model is widely used for modelling the stress flow of the material machined, mainly due to its precision and simplicity.

$$\tau = \sqrt{3}\left[A + B\left(\frac{\gamma}{\sqrt{3}}\right)^n\right]\left[1 + Cln(\dot{\gamma}^*)\right]\left[1 - \left(T^*\right)^m\right] \tag{3.8}$$

where $\dot{\gamma}^*$ is the dimensionless shear strain rate, A is threshold stress in MPa, B is modulus of hardening in MPa, C is the coefficient of sensitivity to strain rate, m is thermal softening coefficient and n is work hardening exponent. The first term in brackets of J-C Eq. 3.8 is elasto-plastic term and represents the strain hardening. The

second one is the vision term and shows that the yield stress flow increases when the material is subjected to high strain rate. The third term is the thermal softening and reflects the fact that the yield stress of material decreases as the temperature increases. The shear strain rate by definition is maximum in shear zone $\dot{\gamma}^* = 1$, which reduces the J-C equation to a function of the effective plastic strain and temperature, reducing with four constants that can be determined as A, B, n and m.

3.3 Results and Discussions

3.3.1 Current density, chip thickness ratio and cutting configurations

In machining, chip formation occurs by imparting shear within a narrow deformation zone called primary shear zone in which the effective strain rates are much larger [75]. The current density which is defined as current intensity through the cross sectional area of the material during cutting, can be considered as an important factor in changing the deformation resistance of material in primary shear zone. The shear cutting area is defined by the segment AB and the length of cutting edge BD (a_b) as shown in Fig. 3.1. The segment AB is described as:

$$AB = \frac{f}{sin(\phi)}, \tag{3.9}$$

ϕ is the shear plane angle (°)

The current density in the primary deformation zone can be calculated by the following equation

$$J_e = \frac{I \cdot \sin(\phi)}{f \cdot a_b}, \tag{3.10}$$

where a_b is the depth of cut. The shear plane angle ϕ proposed in [49] can be expressed geometrically by chip compression ratio ξ as

$$\phi = \arctan\left(\frac{\cos\alpha_0}{\xi - \sin\alpha_0}\right). \tag{3.11}$$

Chip thickness coefficient defined as a ratio $\xi = a_1/a$, where a_1 is deformed chip thickness and $a = f$ is undeformed chip thickness which is actually the feed rate. α_0 is the rake angle which is 6° for the particular tool used during experiments. Chips were collected randomly at the end of each cutting test to measure the thickness of the chip. The chip thickness was measured by using micrometer with 0.01 mm precision. At least 5 measurements were taken to get the average chip thickness. The spindle velocity was measured in rpm with a conventional tachometer. Table table 3.5 gives the values of current densities, chip compression ratio ξ and shear plane angle ϕ with and without pulses as a function of feed rates, cutting velocity and depth of cut for

Table 3.5: Values of chip compression ratio, shear plane angle and current densities as a function of feed rates and cutting speed for steel S235.

Material St S235	Workpiece diameter [mm]	Feed rates (f) [mm/ rev]	Cutting speed (V_c) [m/min]	Depth of cut (a_b) [mm]	Chip compression ratio (ξ)	Shear angle (ϕ) [°]	Current density (J_e) [A/mm^2]
Without pulses	20	0.07	38.213	0.2	6.357	9.037	-
	20	0.14	38.213	0.2	4.321	13.270	-
	20	0.07	57.461	0.2	3.685	15.520	-
	20	0.14	57.461	0.2	2.957	19.220	-
	20	0.07	38.213	0.4	5.257	10.924	-
	20	0.14	38.213	0.4	3.343	17.072	-
	20	0.07	57.461	0.4	4.085	14.025	-
	20	0.14	57.461	0.4	3.057	18.815	-
With pulses	20	0.07	38.213	0.2	3.1	18.366	3151
	20	0.14	38.213	0.2	2.492	22.607	1922
	20	0.07	57.461	0.2	3.171	17.966	3084
	20	0.14	57.461	0.2	2.557	22.072	1878
	20	0.07	38.213	0.4	4.214	13.603	1176
	20	0.14	38.213	0.4	4.228	13.558	586
	20	0.07	57.461	0.4	4.128	13.882	1199
	20	0.14	57.461	0.4	3.378	16.896	726

steel S235.

It can be seen in table 3.5 that chip compression ratio ξ decreases with the increase in feed rates and cutting speed during turning of steel S235. Also the shear plane angle ϕ increases as chip compression ratio ξ decreases. However, as compared to conventional turning process, the values of chip compression ratio ξ are less during electrically assisted turning process. The low values of chip thickness ratio ξ (high ϕ values) mean low shear strain in the shear plane [36]. Since, chip compression ratio ξ is measure of plastic deformation of material which decreases with the increase in cutting speed [27]. Hence, an increase in cutting speed leads to a decrease of plastic deformation in chip formation zone. It was generally observed that the chip thickness decreased as the cutting speed increased and the region of plastic deformation becomes smaller which ultimately reduces the energy consumption [76]

The current density decreases with the increase in feed rates during electrically as-

Table 3.6: Values of chip compression ratio, shear plane angle and current densities as a function of feed rates and cutting speed for Aluminium 6060.

Material Al 6060	Workpiece diameter [mm]	Feed rates (f) [mm/ rev]	Cutting speed (V_c) [m/min]	Depth of cut (a_b) [mm]	Chip compression ratio (ξ)	Shear angle (ϕ) [°]	Current density (J_e) [A/mm^2]
Without pulses	20	0.07	38.213	0.2	2.371	23.691	-
	20	0.14	38.213	0.2	1.214	41.872	-
	20	0.07	57.461	0.2	3.771	15.176	-
	20	0.14	57.461	0.2	2.214	25.241	-
	20	0.07	38.213	0.4	4.028	14.223	-
	20	0.14	38.213	0.4	2.085	26.664	-
	20	0.07	57.461	0.4	5.285	10.867	-
	20	0.14	57.461	0.4	2.971	19.134	-
With pulses	20	0.07	38.213	0.2	3.514	16.261	2800
	20	0.14	38.213	0.2	1.114	44.572	3509
	20	0.07	57.461	0.2	5	11.483	1990
	20	0.14	57.461	0.2	2.914	19.493	1688
	20	0.07	38.213	0.4	3.971	14.424	1245
	20	0.14	38.213	0.4	2.085	26.173	1102
	20	0.07	57.461	0.4	8.628	6.655	579
	20	0.14	57.461	0.4	2.914	19.493	834

sisted turning process of carbon steel as shown in table 3.4. However, the results are in agreement with the previous study [77], in which current density decreases with the increase in feed rates during electrically assisted drilling process. As the chip formation zone decreases with increase cutting speed, this may be the reason why current density values are higher at high cutting speeds for steel S235 during electrically assisted turning process.

Table 3.6 gives the values of chip compression ratio ξ, shear plane angle ϕ and current densities with and without pulses as a function of feed rates, cutting velocity and depth of cut for aluminium 6060. The table 3.6 shows that chip compression ratio ξ decreases with increase in feed rates and increases with the increase in cutting speed. Also shear plane angle ϕ increases with the increase in feed rates and decreases with the increase in cutting speed. The high values of chip compression ratio ξ mean large amount of strain in shear plane [36]. An increase in the cutting speed leads to an increase in the temperature of the chip so its plastic deformation increases [27]. Hence,

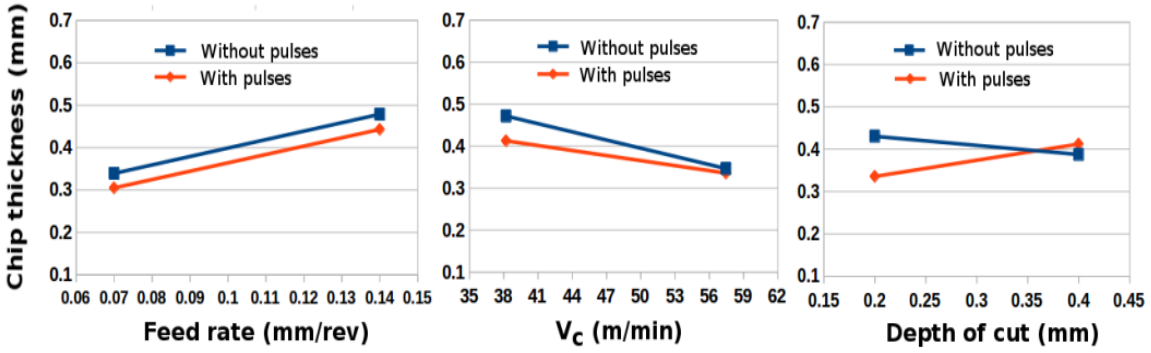

Figure 3.4: Variation of chip thickness with feed rate, cutting speed and depth of while turning steel S235 with and without pulses.

during turning of aluminium 6060, an increase in cutting speed tends to increase chip compression ratio ξ which indicates severe plastic deformation in the chip formation zone.

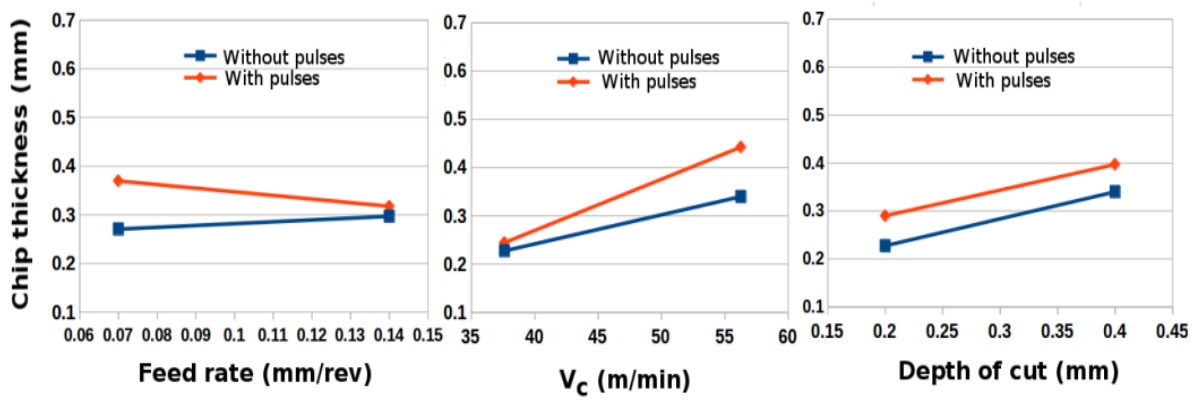

Figure 3.5: Variation of chip thickness with feed rate, cutting speed and depth of while turning aluminium 6060 with and without pulses.

It is also seen in table 3.6 that during electrically assisted turning process the values of chip compression ratio ξ are higher and that of shear plane angle ϕ are lower than conventional turning process in aluminium 6060. Also the current density decreases with the increase in cutting speed while increases with the increase in feed rates.

The Fig. 3.4 demonstrates the variation of chip thickness with feed rates, cutting speed and depth of cut for steel S235 by using factorial analysis. The chip thickness increases with the increase in feed rates and decreases with the increase in cutting speed. The increase in undeformed chip thickness with increasing feed rates will result in increase of shear plane area [59]. The reduction in chip thickness will result in shorter shear plane and longer shear plane is associated with thicker chip produced during the cutting process [78]. However, depth of cut has very little effect on chip

thickness during conventional turning process but chip thickness increases with the increase in depth of cut during EPs assisted turning process.

The Fig. 3.5 shows that feed rates have very little effects on chip thickness, however chip thickness increases with the increase in cutting speed and depth of cut during turning of aluminium 6060. As compared to conventional process, the chip thickness values are higher during electrically assisted turning process. When the chip thickness increases, the chip compression ratio ξ also increases which means plastic deformation of material increases and amount of energy required to accomplish the cutting process of aluminium 6060 also increases.

3.3.2 Specific cutting energy, SCE

The machinability of material can be estimated by comparing the SCE during EP assisted and conventional turning processes. An energy analyzer was developed to measure the power consumption during cutting process. The net effective cutting power consumed N_c (W) is determined by taking the difference between the average power to cut the workpiece and the power of machine without cutting. The net power obtained during conventional turning process is then compared with the power obtained in electrically assisted turning process.

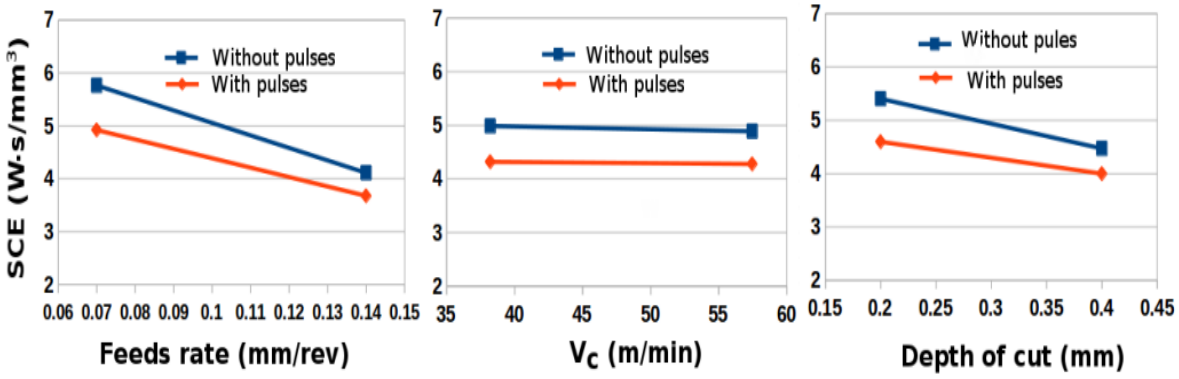

Figure 3.6: Variation of SCE with feed rate, cutting speed and depth of while turning steel S235 with and without pulses.

The Fig. 3.6 showed that the SCE decreased with the increase in feed rates and depth of cut for steel S235 by using factorial analysis. It was observed that the effect of cutting speed on SCE is negligible for steel S235. However, the SCE decreased due to the application of EPs during cutting. The reduction in SCE was observed 7% for high feed rates and 14.62% for low feed rates, 12.46% for high cutting speed and 10.57% for low cutting speed and 10.55% for high depth of cut and 12.11% for low depth of cut. Hence, due to thermal contribution of EPs, the deformation resistance decreases [48],

which ultimately decreases the SCE and improves the plasticity of material during EP assisted turning process. The results are also in agreement with Sànchez et al. [43] and Hameed et al. [77] where the SCE decreases due to the application of electropulses during machining processes.

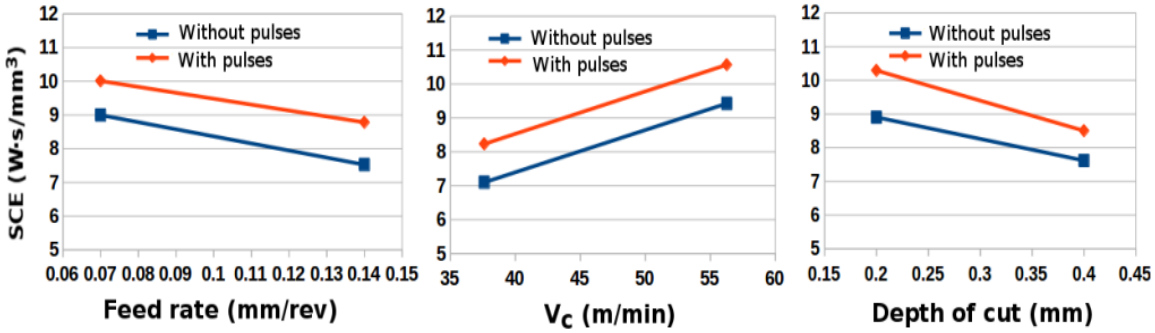

Figure 3.7: Variation of SCE with feed rate, cutting speed and depth of while turning aluminium 6060 with and without pulses.

The Fig. 3.7 presented that SCE decreased with the increase in feed rates and depth of cut for aluminium 6060 by using factorial analysis. However, as compared to steel S235, a different trend was observed when the cutting speed increased the SCE also increased. It is also noted that SCE increased due to the application of EPs during cutting. The cutting at high speed increases the SCE of materials with much higher thermal conductivity and less thermal softening effect [73]. Since aluminium 6060 has higher thermal conductivity and less thermal softening effect as compared to steel S235. So, at higher cutting speed and due to the application of EPs, the strain rate in the shear zone is expected to be high. Thus more heat energy will be generated and time for heat dissipation decreases, which ultimately increases the temperature [79]. Also an excess of electrons can increase the flow stress during superplastic deformation of aluminium alloy [80]. Hence, due to increase of temperature and flow stress, the plastic deformation of material increases which increases the SCE in aluminium 6060.

It can be observed that by increasing the cutting speed for steel S235, the chip thickness decreases and current density increases, while for aluminium 6060, by increasing the cutting speed, chip thickness increases and current density decreases, due to which SCE increases during turning of aluminium 6060 due to the application of EPs. It is assumed that area of deformation zone decreases by increasing the cutting speed for steel S235 and increases by increasing the cutting speed for aluminium 6060. So, it is expected that as compared to steel S235, plastic deformation increases with the increase in cutting speed for aluminium 6060 because of increase of temperature in the chip formation zone.

3.4 Conclusion

The effect of electropulsing has been observed for steel S235 and aluminium 6060 during turning process. Correlation between chip compression ratio ξ, shear plane angle ϕ and current density were obtained by using different cutting parameters for both materials.

The chip compression ratio decreases and shear plane angle increases with the increase in cutting speed during turning of steel S235. In contrast, chip compression ratio ξ increases and shear plane angle ϕ decreases with the increase in cutting speed while turning of aluminium 6060. The current density decreases with the increase in feed rates and increases with the increase in cutting speed in steel S235. However, current density has high values at higher feed rates and it decreases with the increase in cutting speed during turning of aluminium 6060.

The SCE decreased with the increase in feed rates, cutting speed and depth of cut during electrically assisted turning process of steel S235. But a different trend was observed when the cutting speed increased, SCE also increased for aluminium 6060. It is also noted that as compared to steel S235, SCE values are higher in aluminium 6060 when current pulses are induced during turning.

The electrically assisted turning process seems to have influence on improving the machinability of material for steel S235 but for aluminium 6060, plastic deformation tends to be increased. Further investigations are required by studying the chip morphology of S235 steel and aluminium 6060 to further analyze the effect of electropulses on machinability of materials.

3.5 Future work

The study of material deformation in the chip formation zone by using Johnson-Cook constitutive plastic flow stress model (discussed in section 3.2) is still under investigation. The model constitutes the effects of strain hardening, strain rates and thermal softening. The material parameters A, B, m and n can be determined by using flow stress data obtained from mechanical tests.

Chapter 4

General discussion

The purpose of EPs with short duration and high frequency is to soften the material in order to reduce the deformation resistance and increase the plasticity at the same time during metal cutting processes. In this chapter it is tried to discuss the limitations and results obtained during electrically assisted cutting processes to determine the mechanism by which machinability of material can be improved. The SCE which is the indication of machinability of material has been measured and compared for different materials during conventional and electrically assisted cutting processes. Generally, it is expected that when the deformation region is activated by EPs, the current density is favourably directed to minimize the plastic deformation of material in the deformation zone which helps to improve the machinability of material.

As a whole, from the experiments carried out in this thesis, the most important factors which need to discuss are thermal effects, current density threshold and electrical resistivity of materials.

Thermal effects and current density threshold

In machining, the course of rise of temperature in the deformation zone can be regarded as an adiabatic course in a very short time during the EPT. Due to the adiabatic rise of temperature by joule heating effect, the plastic deformation of metals becomes easier. In Chapter 2, the thermal balance approach can be achieved to determine the thermal contribution when short pulses of electricity are induced in 7075 Al and 1045 steel. By considering steady state conditions, the internal thermal energy that can be transferred to its boundary is estimated as:

$$Q_J = \forall \cdot D \cdot C_p \cdot \Delta T, \tag{4.1}$$

Where Q_J is the internal thermal variation of the specimen, $\forall$ is the specimen volume, D is the density of material, C_p is the specific heat capacity and ΔT is the temperature difference.

While the energy generation due to the electric resistance heating is

$$Q_J = I^2 \cdot R \tag{4.2}$$

where I is the current intensity through the specimen and R is the material electric resistance. The thermal contribution by Joule effect due to induced EPs is explained as:

$$Q_J = I^2 \cdot R \cdot t_p . f \tag{4.3}$$

where t_p is the current impulse duration and f is the frequency discharge of current pulse. Comparing the thermal contributions induced by Joule effect and internal thermal variation of the specimen, the following expression is obtained

$$\forall \cdot D \cdot C_p \cdot \Delta T = I^2 . R . t_p . f \tag{4.4}$$

The thermal expansion when short pulses are induced can be written as:

$$\Delta T = (D \cdot C_p)^{-1} \cdot I^2 \cdot \frac{R}{\forall} \cdot t_p . f \tag{4.5}$$

Assuming that the cross sectional area is constant then the above equation can be written as:

$$\Delta T = (D \cdot C_p)^{-1} \left(\frac{I}{A} \right)^2 \cdot \rho . t_p \cdot f \tag{4.6}$$

where A is the cross sectional area and $\rho = \frac{R.A}{L}$ is material resistivity.

Thermal stress distribution

Due to inhomogeneous rise of temperature, inhomogeneous thermal expansion occurs in the area with defects. So thermal stress exists even in the case of uniform temperature distribution and free expansion.

To calculate thermal stress relaxation, lets assume t^* is a dimensionless temperature rise $t^* = \Delta T(t)/\Delta T_{max}$, where $\Delta T(t)$ is the instant temperature change, $\Delta T_{max} (= T_f - T_0)$ is the maximum temperature change; l(t) is the dimensionless thermal expansion,$l(t) = \frac{\Delta L(t)}{\Delta L_{max}}$, where $\Delta L(t)$ is the instant thermal expansion, ΔL_{max} is the maximum thermal expansion. Hence

$$\Delta L_{max} = \alpha \cdot \Delta T_{max} \cdot L_0 \tag{4.7}$$

where α is the coefficient of thermal expansion of specimen and L_0 is the initial length.

When deformation occurs in heated elastic bodies, then from the Duhamal-Neumann relation the thermal stress and strain have the following relation;

$$\sigma_{ik} = \frac{1}{(1+\nu)[E\varepsilon_{ik} + \nu\delta_{ik}s^* - \alpha\Delta T(t)E\delta_{ik}]} \tag{4.8}$$

where

$$s^* = \sigma_{xx} + \sigma_{yy} + \sigma_{zz} \tag{4.9}$$

and ν is the poisson ratio, E is Young's modulus, ε_{ik} is the strain tensor, σ_{ik} is the stress tensor and $delta_{ik}$ is Kronecker delta.

We can suppose that stresses in the transverse directions are zero i,e $\sigma_{yy} = \sigma_{zz} = 0$ for the direction along the length, Eq. 4.8 can be written as

$$\sigma_x(t) = \frac{1}{(1+\nu)[E\varepsilon_x(t) + \nu\sigma_x(t) - \alpha\Delta T(t)E]} \tag{4.10}$$

or

$$\sigma_x(t) = E[\varepsilon_x(t) - \alpha\Delta T(t)] \tag{4.11}$$

Because the distribution of temperature is uniform in x direction, so it can be supposed that $\varepsilon_x(t)$ is the same. Then

$$\Delta L(t) = \int_0^{L_0} \varepsilon_x(t)dx = \varepsilon_x(t)L_0 \tag{4.12}$$

i,e

$$\varepsilon_x(t) = \Delta L(t)/L_0 \tag{4.13}$$

By substituting the Eq. 4.13 and relations $t^* = \Delta T(t)/\Delta T_{max}$, $l(t) = \frac{\Delta L(t)}{\Delta L_{max}}$ into Eq. 4.11 we obtained the following expression;

$$\sigma_x(t) = E[\frac{l(t)\Delta L_{max}}{L_0 - \alpha\Delta t^*\Delta T_{max}}] \tag{4.14}$$

From Eq. 4.7 the thermal stress can be obtained as

$$\sigma_x(t) = E\alpha\Delta T_{max}[l(t) - t^*] \tag{4.15}$$

So thermal stress during expansion is

$$\sigma_x^{'}(t) = -\sigma_x(t) = E\alpha\Delta T_{max}[t^* - l(t)] \tag{4.16}$$

The maximum possible thermal stress in the specimen when instantaneous temperature rise occurs can be estimated by considering the dimensionless temperature $t^* = 0$, when t >0 and $t^* = 1$ when t <0. Then the maximum difference of t^* and l(t) is

equal to 1.

The main cause of thermal stress in this condition is the nonsynchronous change of temperature and thermal expansion. The magnitude of thermal stress depends on time difference between temperature rise and thermal expansion and also the power of heating pulse. The bigger the time difference is the bigger the thermal stress is. The maximum possible thermal stress σ_{max} is determined by the power of the heating pulse. If the thermal expansion changes synchronously with temperature i,e $t^* - l(t) = 0$ then the thermal stress will vanish.

The threshold of current density depends on material and cutting process as shown from experimental results carried out in this thesis. Since, higher cutting speeds decrease the area of shear plane while increasing the shear plane angle, so temperature of the cutting system increases which is advantageous for decreasing the mechanical loads because of thermal softening of materials [81]. The temperature rise due to EPs occurs from the change in stress which indicates that the current produces an effect in addition to that due to heating [6]. In chapter 2, it can be seen that adiabatic rise in temperature and hence maximum stresses increase with the increase in current density by decreasing the feed rates which ultimately reduces the SCE during electrically assisted drilling process.

However, in chapter 3, the effect of current density was found different in electrically assisted turning process. The SCE increases in aluminium 6060 as compared to steel S235. Since the average deformation zone temperature for steel is higher than aluminium [82], so it is expected that an increase in current density increases the temperature in the deformation zone during turning of steel S235 which reduces the plastic deformation and hence ultimately reduces the SCE of material. But for aluminium 6060, the increase in current density increases the uneven temperature in the deformation zone which increases the plastic deformation and hence SCE increases during turning process. The effect of electric field suggests that a deficiency of electrons in workpiece material reduces the flow stress whereas, an excess of electrons increases it [80]. From the results carried out in the thesis, it is suggested that the threshold of current density should be lowered during turning of aluminium 6060 to improve the machinability of process.

Electrical resistivity of materials

Electrical resistivity is an intrinsic property which specifies the flow of electric current through given material. A high resistivity indicates how difficult to flow the electric current through material. Since, the resistivity of carbon steel is higher than aluminium alloy, therefore, in steel the current density should increase the adiabatic temperature rise enough so that plastic deformation can be decreased in the deforma-

tion zone during electrically assisted metal cutting processes.

in chapter 3, it was observed that the current density values are very high during turning of carbon steel S235 and aluminium 6060. As aluminium 6060 has low resistivity and high specific heat capacity than steel S235, so the uneven increase of temperature due to high current density increases the plastic deformation of aluminium 6060 and hence increases the SCE. Mai et al. [83] observed that the electrical resistivity of stainless steel 316L increases in electroplastic deformation. Therefore, it is very important to study the electrical resistivity of different materials when specimens are assisted with EPs in cutting processes in order to analyze how the electrical resistivity of materials are affected.

Electroplastic deformation

In machining, it is desired that the strain in the chip formation zone should be as small as possible to reduce the plastic deformation and improves the efficiency of cutting process. The deformation in the shear plane occurs at high strain rates which generate large amount of heat. In the electroplastic deformation of metals, the electric current that flows through the metal interacts with the deformation of metal by means of Joule heating effect, which reduces the flow stress due to electric current density [82]. During superplastic deformation of aluminium alloy, the electric field has been found to decrease the flow stress, reduce strain hardening and increase the strain rate hardening whereas, an excess of electrons can increase the flow stress [83].

In chapter 2, it can be seen that the SCE decreased for both steel 1045 and aluminium 7075 at low values of current density. It seems that the current density was enough to reduce the plastic deformation of materials during electrically assisted drilling process. However, in chapter 3, the effect of high current density was found different for aluminium 6060 as compared to steel S235. The SCE increased for aluminium 6060 and decreased for steel S235 during electrically assisted turning process. Since, aluminium 6060 has low resistivity and high specific heat capacity than steel S235, so current pulses of high density can increase the flow stress by means of Joule heating effect (thermal effect), which ultimately increases the plastic deformation of aluminium 6060. Hence, for materials like aluminium alloys, an excess of electrons (high current density) can reduce the process efficiency. It is suggested that the EPs of low current density can play an important in improving the machinability of aluminium alloys.

Chapter 5

Conclusions, Contributions to work and Future work recommendations

In this chapter, general conclusions and contribution to work are explained regarding this thesis. Moreover, some recommendations on future work are also suggested based on present research carried out in this thesis.

5.1 Conclusion

The following conclusions are drawn based on the research performed in the thesis.

- An automatic feed mechanism, energy analyser and electrical insulation system were designed and manufactured to control feed velocity, calculate the electrical active power consumption and record the desired electrical and mechanical parameters during cutting processes.
- In chapter 2, the electrically assisted drilling process can be considered as feasible technique to improve the plasticity of material by inducing constant current intensity of short pulses in the cutting zone with a minimum possible plastic deformation.
- As compared to conventional drilling process, the power consumption and SCE were reduced during electrically assisted drilling process. The current density decreases by increasing feed rates, while chip compression ratio ξ decreases and shear plane angle ϕ increases.
- In chapter 3, the effect of EPs observed in steel S235 is found to be different than that observed in aluminium 6060 during turning process. The current density decreases with the increase in feed rates and increases with the increase in cutting speed during turning of steel S235 while, in aluminium 6060, the current density increases with the increase in feed rates and decreases with the increase

in cutting speed. Also as compared to conventional turning process of steel S235, chip thickness values are lower during electically assisted turning process but it is opposite in aluminium 6060 where chip thickness values are higher during electrically assisted process.

- In chapter 3, it is also observed that the electrically assisted turning process seems to have influence on improving the machinability of steel S235 by decreasing SCE. However, in aluminium 6060, the values of SCE are higher than conventional process which seems to increase the plastic deformation of material during electrically assisted turning process.

5.2 Research contributions

The present research has contributed to metal cutting processes particularly electrically assisted drilling and turning processes. The contributions that have been achieved are listed below.

- The mechanism has been developed to electrically isolate each metal cutting machine.
- The methodology to study and analyze the electrical and mechanical parameters has been organized.
- Electropulsing assisted metal cutting processes were proved to be feasible to improve the machinability of materials as compared to conventional metal cutting processes. The results obtained during research either have been published or under consideration. "Electroplastic cutting influence on power consumption during drilling process" [78].

5.3 Future work and recommendations

By considering the conclusions of research described in the thesis, the following recommendations for future work are suggested.

a. Current density and workpiece material.

In chapter 2, the effect of current density seemed to be similar for both aluminium 7075 and steel 1045 as SCE decreased during elctrically assisted drilling process. However, this was not the case during electrically assisted turning process as discussed in chapter 3, where electroplastic effect was different for aluminium 6060 as compared to steel S235 when current pulses of high densities were induced during turning process. Since, aluminium 6060 has low resistivity and high specific heat capacity than steel S235. It is assumed that due to high current density, the adiabatic rise of temperature

increased due to joule heating effect which increases the plasticity of aluminium 6060. Further experiments are necessary to investigate the effect of current densities and subsequently the thermal effects for different materials with different cutting processes.

b. Tool life.

The improvement in efficiency of machining processes is fairly significant which needs further study. Another significant cost of machining processes is the tooling cost associated with worn or chipped cutting tools. If the EPs increase the SCE for aluminium 6060 during turning process, this would be a direct cost increment. It is expected that if cutting forces are increased or decreased during electroplastic metal cutting processes, the tool life can be increased or decreased depending on workpiece material or machining process. It is speculated that there are two possible effects if the cutting tool material is influenced by EPs which would be an interesting follow-on study associated with future work.

1. The EPs may reduce the hardness of cutting tool tending to decrease wear life time.
2. The EPs may increase the toughness of cutting tool tending to increase the toughness and reduce the tendency for chipping the cutting tool and increase tool life.

c. Head effected zone.

It would be worthwhile to examine superficial hardness if the machining surfaces of workpiece materials are different for conventional and assisted drilling processes. If the EPs have potential to change the material being removed like "head effected zone" expect that it would be an "electropulse effected zone".

d. Metallography.

As in chapter chp3, it is seen that the effect of EPs is different for aluminium 6060 and steel S235, it is necessary to study the metallographic observation of different materials assisted by different electrical configurations to analyze the behaviour of materials. It is also important to investigate if EPs can induce the phase transformations, annihilation and accumulation of dislocations, material texture and recrystallization to chipped materials under study. This may help to understand how thermal effects can change the behaviour of chip formation during electrically assisted machining processes.

Appendix A

Configurations of machining operation

A.1 Electroplastic drilling machine

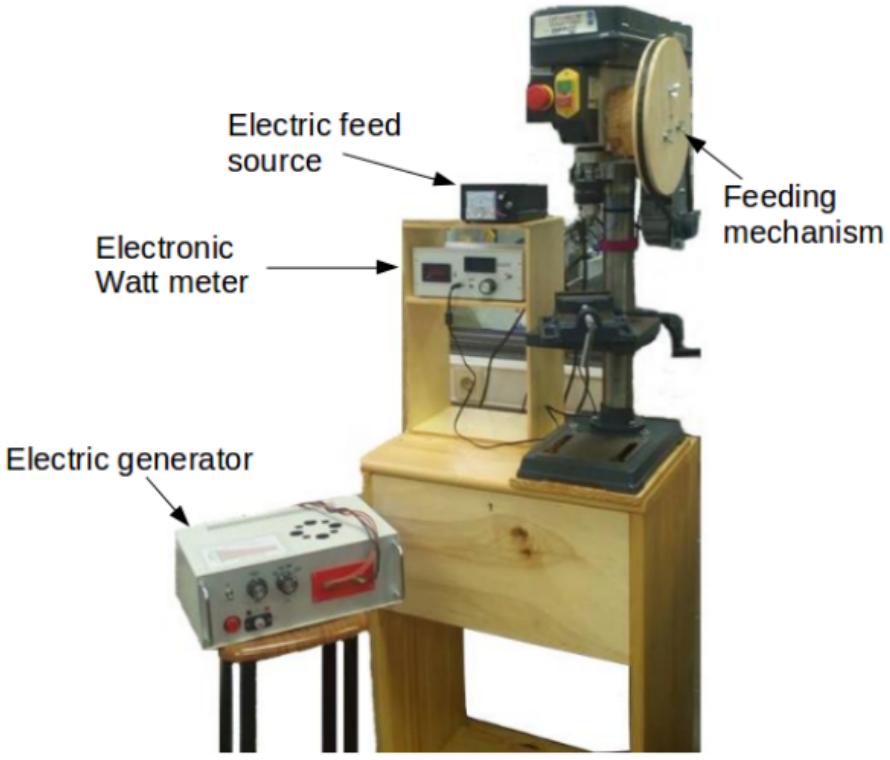

Figure A.1: Electroplastic drilling machine.

It is a small light weighted machine designed for drilling small holes in light jobs for conventional and non conventional processes. It is equipped with an automatic feed mechanism, energy analyzer, source to control feed velocity and an electric pulse

generator as shown in Fig. A.1. The machine has the capacity to rotate drills from 1 to 6 mm at maximum speed of 800 rpm.

Automatic feeding mechanism

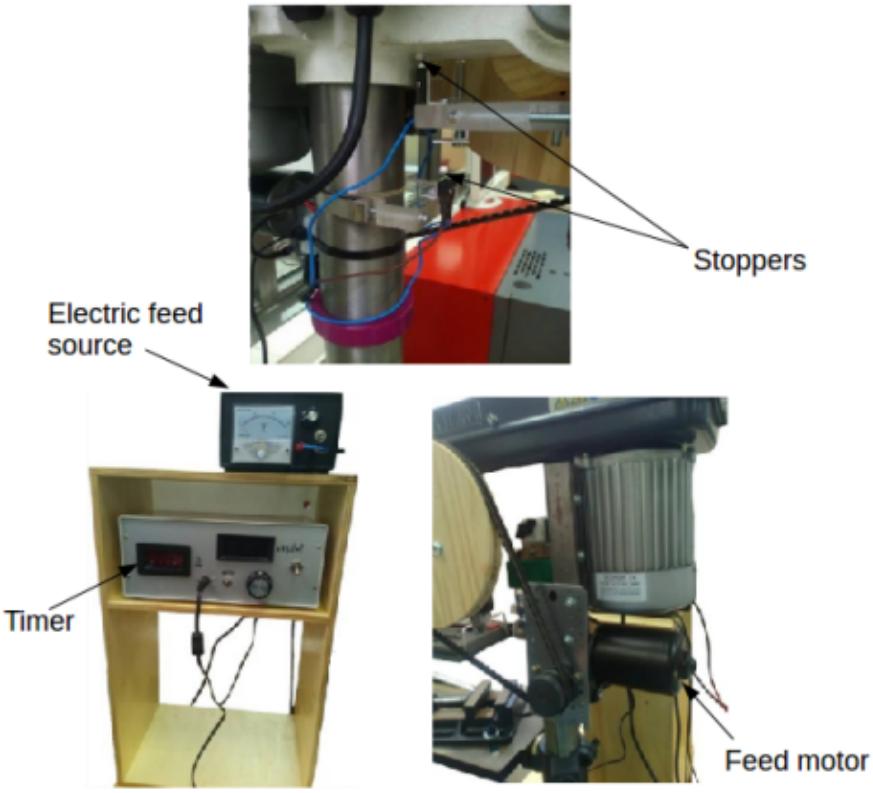

Figure A.2: Automatic feed mechanism.

There is an automatic feed mechanism for feeding the tool into the work piece. The drilling head can be controlled automatically by using an electric feed source linked with a feed motor. This enabled to measure the feed velocity V_f by using stoppers with a distance of 5 mm and the drilling time was measured electronically with the help of timer as shown in Fig. A.2.

Electronic Watt meter

A self made electronic Watt meter linked to drilling motor is used to calculate the electrical active power consumed during drilling as shown in Fig. A.3.

A.2 Mechanical efficiency in turning

The mechanical power N_m produced is proportional to rotational speed and torque. The torque is proportional to load drop across the load arm. It can be increased by increasing the load drop. For an ideal motor, the effective electric power N_e input

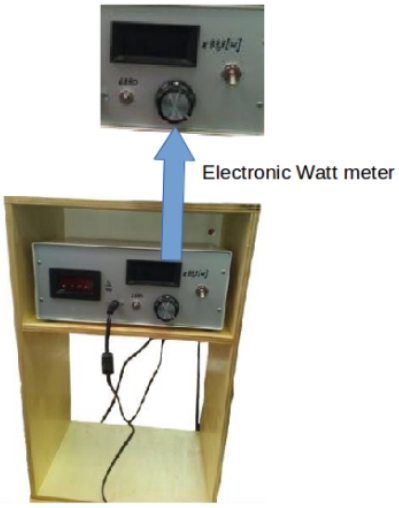

Figure A.3: Electronic Watt meter

equals to cutting power out put i,e $N_e = N_m$. However, practically real motors are not perfectly efficient. So by using calculus to get area under the curve, the mechanical power N_m as a function of effective electrical power N_e can be expressed as

$$N_m = f(N_e) \tag{A.1}$$

The mechanical power of motor for this particular case can be calculated experimentally by measuring the output parameters i,e load drop, load arm and rotational speed as shown in Fig. A.4.

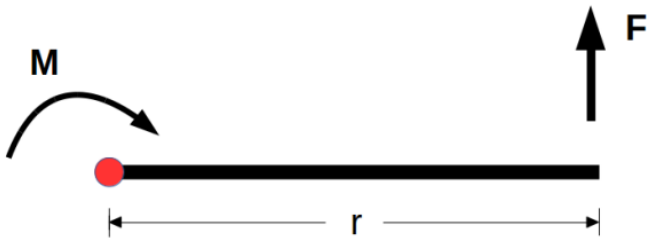

Figure A.4: Evolution of load drop and load arm.

The mechanical power N_m can be estimated as

$$N_m = \tau \cdot \omega \tag{A.2}$$

$$N_m = F \cdot r \cdot \omega \tag{A.3}$$

where F is the load drop in (N), r is load arm in (m) and ω is rotational speed in (rad/sec).

The consumption of energy varies significantly as the cutting tool progresses. The cutting tool requires more power as the volume of the metal being removed increases. Energy efficiency also influences the life and maintenance of tool. The machine tool base load consumes energy even in non-productive phases. So it is necessary to calculate the base load in order to find the exact value of electrical power consumption during machining. This electrical power is then converted into mechanical power which is actually the cutting power.

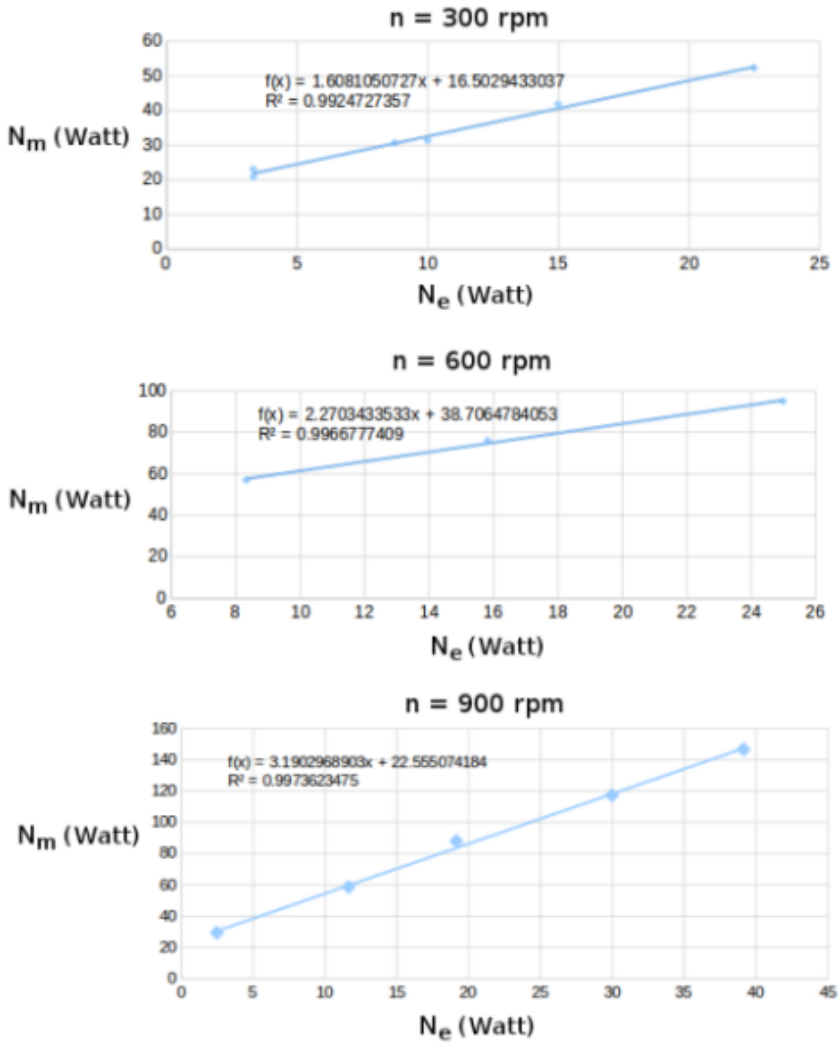

Figure A.5: Relation between mechanical and electrical power of drilling machine.

The Fig. A.5 shows the relation between the mechanical power, N_m and effective electrical power, N_e of turning machine with spindle speeds of 300, 600 and 900 rpm at different loading conditions. The purpose of equation of lines is to estimate the effective

cutting power (mechanical power) for different values of electrical consumption during experiments in turning process.

Bibliography

[1] Guan L, Tang G, and Chu PK, "Recent advances and challenges in electroplastic manufacturing processing of metals," *Journal of Materials Research* Vol. 25 (2010) 1215–1224.

[2] Troitskii OA, "Electromechanical effect in metals," *ZhETF Pisma Redaktsiiu* 10 (1969) 18. http://adsabs.harvard.edu/abs/1969ZhPmR..10...18T.

[3] Conrad H, "Effects of electric current on solid state phase transformations in metals," *Materials Science and Engineering A* Vol. 287 no. 2, (2000) 227–237.

[4] Hui S, and Zhong-Jin W, "Effect of electropulsing on dislocation mobility of titanium sheet," *Transaction of Nonferrous Metals Society of China* Vol. 22 (2012) 1599-1605.

[5] Conrad H, "Space charge and the dependence of the flow stress of ceramics on an applied electric field," *Scripta materialia* Vol. 44 no. 2 (2001) 311–316.

[6] Okazaki K, Kagawa M, and Conrad H, "An evaluation of the contributions of skin, pinch and heating effects to the electroplastic effect in titatnium," *Materials Science and Engineering* Vol. 45 no. 2 (1980) 109–116.

[7] Sprecher AF, Mannan SL, and Conrad H, "Overview no. 49: On the mechanisms for the electroplastic effect in metals," *Acta Metallurgica* Vol. 34 no. 7 (1986) 1145–1162.

[8] Tang G, Zhang J, Yan Y, Zhou H, and Fang W, "The engineering application of the electroplastic effect in the cold-drawing of stainless steel wire," *Journal of Materials Technology* Vol. 137 (2003) 96-99.

[9] Hui S, Zhong-Jin W, and Tie-Jun G, "Effect of high density electropulsing treatment on formability of TC4 titanium alloy sheet," *Transaction of Nonferrous Metals Society of China* Vol. 17 (2007) 87-92.

[10] Zhang W, Sui ML, Zhou YZ, and Li DX, "Evolution of microstructures in materials induced by electropulsing," *Micron* Vol. 34 (2003) 189-198.

[11] Tang DW, Zhou BL, Cao H, and He GH, "Thermal stress relaxation behaviour in thin films under transient laser-pulse heating," *Journal of Applied Physics* Vol. 73 no. 8 (1993) 3749-3752.

[12] Jiang Y, Tang G, Shek C, Xie J, Xu Z, and Zhang Z, "Mechanism of electro-pulsing induced recrystallization in a cold-rolled Mg-9Al-1Zn alloy," *Journal of Alloys and Compounds* Vol. 536 (2012) 94-105.

[13] Xu Z, Tang G, Tian S, Ding F, and Tian H, "Research of electroplastic rolling of AZ31 Mg alloy strip," *Journal of Materials Processing Technology* Vol. 182 (2007) 128-133.

[14] Xu Q, Tang G, Jiang Y, Hu G, and Zhu Y, "Accumulation and annihilation effects of electro-pulsing on dynamic recrystallization in magnesium alloy," *Materials Science and Engineering A* Vol. 528 (2011) 3249-3252.

[15] Molotskii M and Fleurov V, "Magnetic effects in electroplasticity of metals," *Physical Review B* Vol. 52 no. 22, (1995) 15829.

[16] Zhu R, Tang G, Shi S, and Fu M, "Effect of electroplastic rolling on deformability and oxidation of NiTiNb shape memory alloy," *Journal of materials processing technology* Vol. 213 (2013) 30-35.

[17] Tao B, Liu J, and Li S,"Oxidaton behaviors of $Ti_{44}Ni_{47}Nb_9$ shape memory alloy at high temperature," *Acta Metallurgica Sinica* Vol. 41 (2005) 633–637.

[18] Xu ZH, Tang GY, Tian SQ, Ding F, and Tian HY,"Research of electroplastic rolling of AZ31 Mg alloy strip," *Journal of Material Processing Technology* Vol. 182 (2007) 128-133.

[19] Jiang Y, Guan L, Tang G, Shek C, and Zhang Z, "Influence of electro-pulsing treatment on microstructure and mechanical properties of cold rolled Mg-9Al-1Zn alloy strip," *Materials Science and Engineering A* Vol. 528 (2011) 5627-5635.

[20] Hui S and Zhong-Jin W, "Improvement of mechanical properties of cold-rolled commercially pure Ti sheet by high density electropulsing," *Transaction of Nonferrous Metals Society of China* Vol. 22 (2012) 1350-1355.

[21] Hui S and Zhong-Jin S, "Grain refinement by means of phase transformation and recrystallization induced by electropulsing," *Transaction of Nonferrous Metals Society of China* Vol. 21 (2011) 353-357.

[22] To S, Zhu YH, Lee WB, Liu XM, Jiang YB and Tang GY, "Effects of current density on electropulsing-induced phase transformations in a Zn–Al based alloy," *Applied Physics A* Vol. 96 (2009) 939–944.

[23] Zhang D, To S, Zhu Y, Wang H and Tang G, "Dynamic electropulsing induced phase transformations and their effects on single point diamond turning of AZ91 alloy," *Journal of Surface Engineered Materials and Advanced Technology* Vol. 2 (2012) 16-21.

[24] Yao K, Wang J, Zheng M, Yu P and Zhang H, "A research on electroplastic effects in wire drawing process of an austenitic stainless steel," *Scripta Materialia* Vol. 45 (2001) 533-539.

[25] Tang G, Zheng M, Zhu Y, Zhang J, Fang W and Li Q, "The application of the electro-plastic technique in the cold-drawing of steel wires," *Journal of Materials Processing Technology* Vol. 84 (1998) 268 – 270.

[26] Tang G, Zhang J, Zheng M, Zhang J, Fang W and Li Q, "Experimental study of electroplastic effect on stainless steel wire 304L," *Materials Science and Engineering A* Vol. 281 (2000) 263 – 267.

[27] Astakhov VP, and Shvets S, "The assessment of plastic deformation in metal cutting," *Journal of Materials Processing Technology* Vol. 146 (2004) 193-202.

[28] Astakhov VP, Drills: Science and Technology of Advanced Operations, CRC Press, Taylor and Francis Group (2014).

[29] Pervaiz S, Deiab I, Rashid A, Nicolescu M, Kishawy H, "Energy consumption and surface finish analysis of machining Ti6Al4V," *International Scholarly and Scientific Research & Innovation* Vol. 7(4) (2013) 535-540.

[30] Neugebauer R, Schubert A, Reichmann B, Dix M, " A study on energy efficiency improvement for machine tools," *CIRP Journal of Manufacturing Science and Technology* Vol. 4 (2011) 161–169.

[31] Simoneau A, Meehan J, "The Impact of machining parameters on peak power and energy consumption in CNC endmilling," *Energy and Power* Vol. 3(5) (2013) 85-90.

[32] Bhattacharya A, Das S, Majumder P, Batish A, "Estimating the effect of cutting parameters on surface finish and power consumption during high speed machining of AISI 1045 steel using Taguchi design and ANOVA," *Production Engineering. Research and Development* Vol. 3 (2009) 31–40.

[33] Fernández-Abia AI, Barreiro J, López de Lacalle LN, and Martínez S, "Effect of Very High Cutting Speeds on Shearing, Cutting Forces and Roughness in Dry Turning of Austenitic Stainless Steels," *International Journal of Advanced Manufacturing Technology* Vol. 57 (2011) 61–71.

[34] Draganescu F, Gheorghe M, Doicin CV, "Models of machine tool efficiency and specific consumed energy," *Journal of Material Processing Technology* Vol. 141 (2003) 9–15.

[35] Mativenga PT, and Rajemi MF, "Calculation of optimum cutting parameters based on minimum energy footprint," *CIRP Annals - Manufacturing Technology* Vol. 60 (2011) 149-152.

[36] Silva LR, Abrão AM, Faria P, Davim JP, "Machinability study of steels in precision orthogonal cutting," *Materials Research* Vol. 15(4) (2012) 589-595.

[37] Mori M, Fujishima M, Inamasu Y, and Oda Y, "A study on energy efficiency improvement for machine tools," *CIRP Annals - Manufacturing Technology* Vol. 60 (2011) 145-148.

[38] Yoon HS, Moon JS, Pham MQ, Lee GB, Ahn SH, "Control of machining parameters for energy and cost savings in micro-scale drilling of PCBs", *Journal of Cleaner Production* Vol. 54 (2013) 41-48.

[39] Hamade RF, and Ismail F, "A Case for Aggressive Drilling of Aluminum," *Journal of Materials Processing Technology* Vol. 166 (2005) 86–97.

[40] Zhang J, Tang G, Yan Y, and Fang W, "Effect of current pulses on the drawing stress and properties of Cr17Ni6Mn3 and 4J42 alloys in the cold-drawing process," *Journal of Materials Processing Technology* Vol. 120 (2002) 13-16.

[41] ZHANG D, TO S, ZHU Y, WANG H and TANG G, "Static electropulsing induced microstructural changes and their effect on the ultra-precision machining of cold Rolled AZ91 alloy," *Metallurgical and Materials Transactions A* Vol. 43A, (2012) 1341-1346.

[42] Baranov SA, Staschenko VI, Sukhov AV, Troitskiy OA, Tyapkin AV, "Electroplastic Metal Cutting," *Russian Electrical Engineering* Vol. 82 (2011) 477-479.

[43] Sànchez AJE, Gonzàlez HAR, Montilla CA and Echeverri VK, "Effect of electroplastic cutting on the manufacturing process and surface properties," *Journal of Materials Processing Technology* Vol. 222 (2015) 327-334.

[44] Pu CL, Zhu G, Yang S, Yue EB, Subramanian SV, "Effect of microstructure softening events on the chip morphology of AISI 1045 steel during high speed machining," *International Journal of Advanced Manufacturing & Technology* Vol. 82 (2016) 2149–2155.

[45] Zhao D, and Chaudhury PK, "Effect of starting grain size on As-deformed microstructure in high temperature deformation of alloy 718," *The Minerals, Metals & Materials Society* (1994) 303-313.

[46] Sun S, Brandt M, Song W.Q, Matthew S, Dargusch, "Microstructural evolution in chips during machining of commercially pure (Grade 2) titanium," *Materials Science Forum* Vol. 654-656 (2010) 823-826

[47] Zhang W, Sui ML, Zhou YZ, Li DX, "Evolution of microstructures in materials induced by electropulsing," *Micron* Vol. 34 (2003) 189–198.

[48] Magargee J, Morestin F and Cao J, "Characterization of flow stress for commercially pure titanium subjected to electrically assisted deformation," *Journal of Engineering Materials and Technology* Vol. 135/041003 (2013) 1-10.

[49] Feng K, Jun N and Stephenson DA, "Chip thickening in deep-hole drilling," *International Journal of Machine Tools and Manufacturing* Vol. 46 (2006) 1500–1507.

[50] Du XN, Yin SM, Liu SC, and Wang BQ, "Effect of the electropulsing on mechanical properties and microstructure of an ECAPed AZ31 Mg alloy," *Journal of Materials Research* Vol. 23(06) (2008) 1570-1577.

[51] Stephenson DA, and Agapiou JS, "Metal Cutting Theory and Practice," CRC Press sec ed Taylor and Francis Group (2005).

[52] Ekincioglu G, Altindag R, Sengun N, Demirdag S, and Guney A, "The relationships between drilling rate index (DRI), physico-mechanical properties and specific cutting energy for some carbonate rocks," *Rock Mechanics for Resources, Energy and Environment* Vol. 136 (2013) 867-873.

[53] Boothroyd G, and Knight WA, "Fundamentals of Metal Machining and Machine Tools," Mercel Dekker, Second edition, New York (1989).

[54] Sood R, Guo C, and Malkin S, "Turning of hardened steels," *Journal of Manufacturing Processes* Vol. 2(03) (2000) 187-193.

[55] Edward MT, Metal cutting: *Fourth Edition*, Butterworth–Heinemann (2000).

[56] Astakhov VP, Geometry of single-point turning tools and drills: Fundamentals and Practical Applications (2010).

[57] Astakhov VP, Tribology of metal cutting: Tribology and Interface Engineering Series, 52 Editor: B.J. Briscoe (2006).

[58] Sourabh. P, Bandyopadhyay. pp, and Paul. S, "Minimisation of specific cutting energy and back force in turning of AISI 1060 steel," *Journal of Engineering Manufacture* Proc IMech Part B.

[59] Adam UA, Noordin MY, Mohamed HSE, and Hasan F, "Influence of cutting conditions on chip formation when turning ASSAB DF-3 Hardened tool steel," International *Journal of Materials, Mechanics and Manufacturing*, Vol. 1(1) (2013).

[60] Gui GY, Shi FX, Xing HT, and Lan HD, "Influence of cutting conditions on the cuuting performance of TiAl6V4," *Advanced Material Research*, Vol. 337 (2011) 387-391.

[61] Merchant ME,"Basic mechanics of the metal cutting process," *ASME J Appl Mech* Vol. 66 (1944) 168–175.

[62] Oxley PLB, "A strain-hardening solution for the shear angle in orthogonal metal cutting," *Int J Mech Sci* Vol. 3 (1961) 68–79.

[63] Adibi-Sedeh AH, Madhavan V, and Bahr B, "Extension of Oxley's analysis of machining to use different material models," *J Manuf Sci Eng* Vol. 125 (2003) 656–666.

[64] Lalwani DI, Mehta NK, and Jain PK, "Extension of Oxley's predictive machining theory for Johnson and Cook flow stress model," *J Mater Process Technol* Vol. 209 (2009) 5305–5312.

[65] Tounsi N, Vincenti J, Otho A, and Elbestawi MA, "From the basics of orthogonal metal cutting toward the identification of the constitutive equation. *Int J Mach Tools Manuf* Vol. 42(2) (2002) 1373–1383.

[66] Dudzinski D, Molinari A, "A modelling of cutting for viscoplastic materials," *Int J Mech Sci* Vol. 39(4) (1997) 369–389.

[67] Becze CE, Worswick MJ, and Elbestawi MA, "High strain rate shear evalution and characterization of AISI D2 tool steel in its hardened state," *Machining Science and Technology: An International Journal*, Vol. 5(1) (2001) 131-149.

[68] Boothroyd G, and Bailey JA, "Effects of strain rate and temperature in orthogonal metal cutting," *Journal Mechanical Engineering Science*, Vol. 8(3) (1966) 264-275.

[69] Lee S, Hwang J, Ravi SM, ChandrasEekAar S, and Compton WD, "Large strain deformation field in machining," *Metallurgical and Materials Transactions*, Vol. 37A (2006) 1633—1643.

[70] Oxley FL, Humphreys AG, and Larizadeh A,"The influence of rate of strain hardening in machining," *Proc Inatpl Mech Engrs* Vol. 175(18) (1961) 881-891.

[71] Astakhov VP, and Shvets SV, "A novel approach to operating force evolution in high strain rate metal-deforming technological processes," *Journal of Materials Processing Technology*, Vol. 117 (2001) 226-237.

[72] Hocheng H, Yen SB, Ishihara T, and Yen BK, "Fundamental turning characteristics tribology-favored graphite/aluminum composite material," *Composires Part A* Vol. 28A (1997) 883-890.

[73] Bakkal M, Shih AJ and Scattergood RO, "Chip formation, cutting forces and tool wear in turning of Zr-based bulk metallic glass," *International Journal of Machine Tools & Manufacture*, Vol. 44 (2004) 915-925.

[74] Komanduri R, Hou ZB, "Thermal modeling of the metal cutting process, part I: temperature rise distribution due to shear plane heat source," *International Journal of Mechanical Sciences*, Vol. 42 (2000) 1715–1752.

[75] Deng WJ , Lin P, Xie ZC, and Li Q, "Analysis of large-strain extrusion machining with different chip compression ratios," *Journal of Nanomaterials*, Vol. 2012 (2012) 1-12.

[76] Thamizhmanii S, and Hasan S, "Machinability study using chip thickness ratio on difficult to cut metals by CBN cutting tool," *Key Engineering Materials* Vol. 504-506 (2012) 1317-1322.

[77] Hameed S, Gonzàlez RHA, Sànchez EAJ and Alberro AN, "Electroplastic cutting influence on power consumption during drilling process," *International Journal of Advanced Manufacturing Technology* Vol. 87 (2016) 1835-1841.

[78] Natasha AR, Othman H, Ghani JA, Haron CHC, and Syarif J, "Chip formation and coefficient of friction in turning S45C medium carbon steel," *International Journal of Mechanical & Mechatronics Engineering IJMME-IJENS* Vol. 14 06 (2014) 89-92.

[79] Thakur DG, Ramamoorthy B, Vijayaraghavan L, "A study on the parameters in high-speed turning of superalloy Inconel 718," *Materials and Manufacturing Processes* Vol. 24(4) (2009) 497-503.

[80] Conrad H, Sprecher AF, Cao WD, Lu XP, "Electroplasticity — the effect of electricity on the mechanical properties of metals," *The Journal of The Minerals, Metals & Materials Society* Vol. 42 (1990) 28-33.

[81] Fahad M, Mativenga PT, and Sheikh MA, "On the contribution of primary deformation zone-generated chip temperature to heat partition in machining," *International Journal of Advanced Manufacturing Technology* Vol. 68 (2013) 99–110.

[82] David AS, and John SA, "Metal cutting theory and practice, Third edition," CRC Press Taylor & Francis Group (2016).

[83] Mai J, Peng L, Lin Z, and Lai X, "Experimental study of electrical resistivity and flow stress of stainless steel 316L in electroplastic deformation," *Materials Science and Engineering A* Vol. 528 (2011) 3539–3544.